

# Galaxy groups in the low-redshift Universe

S.H. Lim<sup>1\*</sup>, H.J. Mo<sup>1,2</sup>, Yi Lu<sup>3</sup>, Huiyuan Wang<sup>4</sup>, Xiaohu Yang<sup>5,6</sup>

<sup>1</sup>*Department of Astronomy, University of Massachusetts, Amherst MA 01003-9305, USA*

<sup>2</sup>*Physics Department and Center for Astrophysics, Tsinghua University, Beijing 10084, China*

<sup>3</sup>*Key Laboratory for Research in Galaxies and Cosmology, Shanghai Astronomical Observatory, Nandan Road 80, Shanghai 200030, China*

<sup>4</sup>*Key Laboratory for Research in Galaxies and Cosmology, Department of Astronomy, University of Science and Technology of China, Hefei, Anhui 230026, China*

<sup>5</sup>*Department of Astronomy, Shanghai Jiao Tong University, Shanghai 200240, China*

<sup>6</sup>*IFSA Collaborative Innovation Center, Shanghai Jiao Tong University, Shanghai 200240, China*

Accepted ..... Received .....; in original form .....

## ABSTRACT

We apply a halo-based group finder to four large redshift surveys, the 2MRS, 6dFGS, SDSS and 2dFGRS, to construct group catalogs in the low-redshift Universe. The group finder is based on that of Yang et al. but with an improved halo mass assignment so that it can be applied uniformly to various redshift surveys of galaxies. Halo masses are assigned to groups according to proxies based on the stellar mass/luminosity of member galaxies. The performances of the group finder in grouping galaxies according to common halos and in halo mass assignments are tested using realistic mock samples constructed from hydrodynamical simulations and empirical models of galaxy occupation in dark matter halos. Our group finder finds  $\sim 94\%$  of the correct true member galaxies for 90 – 95% of the groups in the mock samples; the halo masses assigned by the group finder are un-biased with respect to the true halo masses, and have a typical uncertainty of  $\sim 0.2$  dex. The properties of group catalogs constructed from the observational samples are described and compared with other similar catalogs in the literature.

**Key words:** methods: statistical – galaxies: formation – galaxies: evolution – galaxies: haloes.

## 1 INTRODUCTION

Grouping galaxies observed in a galaxy catalog into systems (clusters and groups) is a practice of long history. In the early attempts, clusters of galaxies were identified based on optical photometric data, using the local density contrast of galaxies in the sky as a proxy of spatial density and using distance estimates that are based on galaxy magnitudes. For example, Abell (1958) constructed a catalog of about 2,700 clusters from the POSS plates using local galaxy surface number densities. A similar selection was used by Abell et al. (1989) to construct a catalog of 1,600 clusters from the UKST plates. Zwicky et al. (1961–1968) identified 9,133 clusters in the northern celestial hemisphere using the POSS plates, and adopting a galaxy number density criterion that is relative to the immediate neighborhood. Because these catalogs are constructed from photographic plates and no redshift information is available for individual galaxies, they

suffer severely in in-homogeneity, incompleteness, and projection effects.

With the advent of large redshift surveys in 1980s, a lot of efforts were made to select galaxy clusters/groups on the basis of closeness of galaxies in redshift space. Although differing in details, many of these investigations have adopted the so-called friends-of-friends (FoF) method, which identifies galaxy systems as member galaxies that are linked by some adopted linkage criteria. For example, Postman & Geller (1984) identified galaxy groups from the CfA redshift survey (Huchra et al. 1983) by applying the FoF algorithm, developed by Huchra & Geller (1982), which uses two linking criteria, one on projected separation and the other on redshift difference, to link galaxies. With modifications, the FoF algorithm has been applied to various redshifts surveys of galaxies, including the Two Degree Field Galaxy Redshift Survey (2dFGRS; e.g. Eke et al. 2004), the Two Micron All Sky Redshift Survey (2MRS; e.g. Crook et al. 2007), and the Sloan Digital Sky Survey (SDSS; e.g. Goto 2005; Berlind et al. 2006). Lavaux & Hudson (2011) applied the FoF group

\* E-mail: slim@astro.umass.edu

finder to their own compilation combining the 2MRS, SDSS and Six Degree Field Galaxy Survey (6dFGS).

As high density regions in the galaxy distribution, clusters and groups of galaxies have been widely used to study the environmental dependence of the galaxy population and its evolution. For example, Dressler (1980) found that the morphology of a galaxy is correlated with the local density of galaxies in that the fraction of elliptical galaxies is higher in regions of higher density. Butcher & Oemler (1978, 1984) studied the galaxy populations in rich and compact clusters at redshifts of  $\sim 0.4$  and found that the ratio of blue galaxies is higher than that in nearby clusters of similar richness and morphology, implying a strong recent evolution in galaxy color. Galaxy systems have also been assumed to be associated with dark matter halos. In the 1930s, Zwicky studied the motion of galaxies within the Coma Cluster and found that the total mass of the cluster estimated using the virial theorem is more than 100 times higher than that estimated from the total luminosity of member galaxies. This is the first evidence for the presence of a large amount of non-luminous (dark) matter in clusters of galaxies. While the result was not widely accepted at the time, subsequent observations based on galaxy velocity dispersion, X-ray emission and gravitational lensing effects have provided indisputable evidence that galaxy clusters and groups are all associated with massive dark matter halos. Indeed, even isolated galaxies are also found to be embedded in massive halos, as inferred from their rotation curves and velocity dispersion of stars.

Theoretically, the current  $\Lambda$ CDM model predicts that all galaxies form and evolve in dark matter halos. These halos are virialized clumps of dark matter that form in the cosmic density field through gravitational instability (see Mo et al. 2010, for a review). Therefore, galaxy systems, if selected properly so as to represent halos, can be used to study how galaxies form and evolve in dark matter halos. Furthermore, since dark matter halos are simple but biased tracers of the underlying mass density field (e.g. Mo & White 1996), galaxy systems so selected can also be used to study the structure and evolution of the mass density field in the universe. In particular, as shown in Wang et al. (2009), a well-defined group sample can be used to reconstruct the cosmic density field, which, in turn, can be used to reconstruct the initial conditions from which the observed structures form and evolve (Wang et al. 2013, 2014, 2016).

A key in using galaxy systems as a proxy of the dark halo population is a group finder that can group galaxies according to common dark matter halos. The widely adopted FoF algorithm is not optimal for the purpose. More recently, Yang et al. (2005) (Y05 hereafter) developed a halo-based group finder, which identify groups based on dark matter halo properties, such as mass and velocity dispersion, expected from the CDM cosmogony. This halo-based group finder has been extensively tested using mock galaxies from simulations and found to perform much better than the traditional FoF algorithm, particularly in identifying poor systems. The group finder of Y05 has been applied to redshift surveys such as the 2dFGRS (e.g. Yang et al. 2005), the SDSS (e.g. Weinmann et al. 2006; Yang et al. 2007), and the 2MRS (e.g. Lu et al. 2016). Similarly, Duarte & Mamon (2015) adopted an iterative group membership assignment algorithm but in a probabilistic way using galaxy

distribution statistics extracted from N-body simulation. An important step in the halo-based group finder is the use of a halo-mass proxy to assign halo masses to tentative groups/clusters in the grouping process. Y05 suggested the use of the ranking of the total luminosity of galaxies that have luminosities above a certain value as the proxy of halo mass, and this mass proxy was adopted in the SDSS and 2dFGRS group catalogs mentioned above. However, this mass proxy may not be suitable for shallower surveys, such as the 2MRS, where many systems contain only a small number of galaxies. In order to overcome this limitation, Lu et al. (2016) (L16 hereafter) proposed a ‘‘GAP correction’’ method, in which the luminosity/stellar mass of the most luminous/massive member is combined with the ‘‘GAP’’ to form a mass proxy, where ‘‘GAP’’ is defined to be the difference in luminosity/stellar mass between the most luminous/massive member and  $n$ -th most luminous/massive member. Using a 2MRS mock sample, L16 found that the GAP method yields a typical dispersion of  $\sim 0.3$  dex in the estimated masses for galaxy systems of a given true halo mass.

In this paper, we modify the group finders of Y05 and L16, paying particular attention to the extension of the methods to poor systems, such as groups containing one member or a small number of members, in a uniform way. We use mock samples constructed from numerical simulations and an empirical model to calibrate the halo mass proxies and to test the performances of the group finder under different sample selections. As we will see below, our modified group finder not only gives more accurate halo mass estimates for groups than the original group finders, it also enables us to uniformly extend the group samples to systems with halo masses that are about an order of magnitude lower than in the existing group catalogs. We apply our group finder to a number of redshift surveys in the local universe, including the 2MRS, the 6dFGS, the updated release of SDSS and the 2dFGRS. As mentioned above, group catalogs have been constructed from some of these catalogs with various group finders. Our goal here is to extend, update, and add values to, these catalogs by providing group samples that are uniformly selected from improved data using improved methods.

The outline of this paper is as follows. In Section 2, we describe the observational data to which we apply our group finder, and the simulation that we use to calibrate and test the group finder. Section 3 explains in detail the group finder and how to test and calibrate a variety of halo-mass proxies using mock galaxies. In Section 4, we apply the group finder to the mocks of the same sample selection as the observational data, and assess its performance by comparing halo masses, membership assignments, and global completeness between the constructed mock groups and the simulations. In Section 5, we apply the group finder to real observations, construct our group catalogs, describe their basic properties and how to use them, and make comparisons with other catalogs in the literature. Finally, we summarize our results and discuss applications of the catalogs in Section 6.

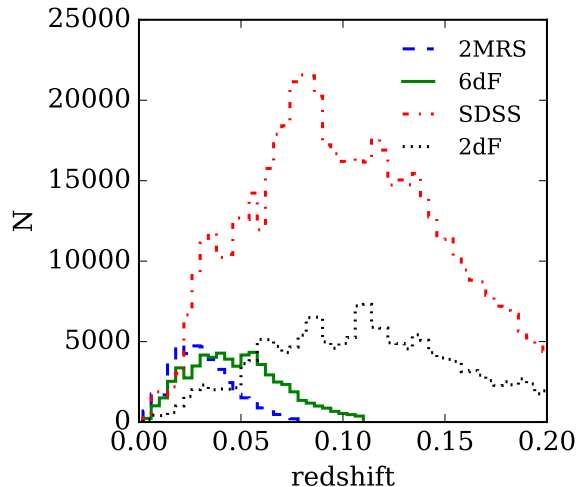


**Figure 1.** The redshift distributions of galaxies in the four samples we use to identify galaxy groups. The bin size of the histograms is  $\Delta z = 0.004$ .

## 2 OBSERVATIONAL DATA AND MOCK SAMPLES

In this section, we describe in detail the galaxy samples we use to construct our group catalogs. Since our goal is to provide well-defined group catalogs in the local universe, we decide to use all major redshift surveys at low redshift ( $z < \sim 0.2$ ) that are publicly available. A brief summary of our sample selections is given in Table 1. The redshift distributions of these samples are shown in Figure 1, and their sky coverages are plotted in Figure 2.

### 2.1 The 2MRS catalog

Our first galaxy sample is selected from the 2MASS Redshift Survey (2MRS; Huchra et al. 2012), which is based on the Two Micron All Sky Survey (2MASS; Skrutskie et al. 2006). 2MASS covers  $\sim 91\%$  of the entire sky in the near-infrared  $J$ ,  $H$ , and  $K_s$  bands. Because of the reduced dust extinction in the NIR, 2MASS is an almost uniform survey down to the magnitude limit  $K_s \leq 13.5$ , except in the region within  $\pm 5^\circ$  of the Galactic plane (the “zone of avoidance” or ZoA). The extended source catalog (the 2MASS XSC) contains  $\sim 10^6$  objects. The 2MRS attempted to obtain redshifts, either from its own observation or from other data bases, for 45,086 sources of the 2MASS XSC that meet the following criteria:

- (i)  $K_s \leq 11.75$  mag and detected at  $H$ ,
- (ii)  $E(B - V) \leq 1$ ,
- (iii)  $|b| \geq 5^\circ$  for  $30^\circ \leq l \leq 330^\circ$ ;  $|b| \geq 8^\circ$  otherwise,

where  $b$  is the Galactic latitude, and  $E(B - V)$  is the extinction based on the dust map of Schlegel et al. (1998). As shown in Huchra et al. (2012), to the magnitude limit  $K_s = 11.75$  the completeness does not change significantly within the region specified by criterion (iii). Of the 45,086 sources, 2MRS rejected a small fraction that is of galactic origin, only partially detected, or not clearly detected due to contamination. This leaves a total of 44,599 galaxies.

The details about the selection can be found in Huchra et al. (2012) and its appendix. For the 44,599 galaxies, 2MRS eventually obtained redshifts for 43,533 systems, achieving a completeness of about 97.6%. These include 11,000 galaxies measured by the 2MRS team, 7,069 galaxies with redshifts from SDSS, 11,763 from 6dFGS DR3, 12,952 from the NASA Extragalactic Database (NED), and 749 from J. Huchra’s personal compilation (ZCAT). For objects with redshifts from more than one source, the preference was given in the order of 2MRS, SDSS, 6dF, NED, and ZCAT.

For the 1,066 galaxies that do not have redshifts from the 2MRS, we either adopt redshifts of their nearest neighbors or use those given by the 2MASS Photometric Redshift catalog (2MPZ; Bilicki et al. 2014). The 2MPZ uses the optical, NIR, and mid-IR photometry from SuperCOSMOS, 2MASS, and WISE respectively, to obtain photometric redshifts for about 1 million galaxies, by employing an artificial neural network approach trained with several redshift surveys. The photometric redshifts obtained have a typical error of 12%. We first assign redshifts of the nearest neighbors ( $z_{NN}$ ) to all galaxies without the spectroscopic redshift. Then, if a galaxy also has a redshift from the 2MPZ ( $z_{pho}$ ) and  $z_{pho}$  differs from  $z_{NN}$  by more than 12%, we assign  $z_{pho}$  as the redshift of the galaxy instead of  $z_{NN}$ .

With all these, we obtain redshifts for 288 additional galaxies from their nearest neighbors, and redshifts for 778 galaxies from the 2MPZ, thus assigning redshifts to all the 44,599 galaxies. Because of the uncertainties in the nearest-neighbor and photometric redshifts, we will provide two separate catalogs: the first is constructed from the sample of galaxies that all have 2MRS redshifts; the second uses all galaxies that have 2MRS redshifts,  $z_{pho}$ , or  $z_{NN}$ . The latter will have a flag that shows source of redshifts for each galaxy, as well as the separation to the nearest neighbor for galaxies with  $z_{NN}$  so that a user can decide an uncertainty that may be allowed to suit his/her scientific goal. For convenience, we refer to the 1st catalog as 2MRS and the 2nd as 2MRS+.

Our sample also contains a number of refinements appropriate for our purpose. First, we correct all the redshifts (radial velocities) of galaxies to the CMB rest-frame. To do this, we assume that the heliocenter is moving with a velocity of 368 km/s towards  $(l, b) = (263.85^\circ, 48.25^\circ)$  with respect to the CMB (Bennett et al. 2003). Second, we only use galaxies with corrected redshifts  $z \leq 0.08$ , which eliminates about 1% of the galaxies from the sample. The final numbers of galaxies are then 43,249 and 44,310 for 2MRS and 2MRS+, respectively. As an example, the redshift and sky distributions of the galaxies in 2MRS are shown in Figures 1 and 2, respectively, and a brief summary of the samples is given in Table 1.

We use the extinction-corrected  $K_s$  isophotal magnitudes from the 2MRS. The extinction-correction accounts for dust extinctions of the Milky Way relying on the dust map by Schlegel et al. (1998). We use WMAP9 cosmology to convert apparent magnitudes to absolute magnitudes in a bandpass  $Q$  as followings:

$$M_Q = m_Q + \Delta m_Q - DM(z) - K_Q(z) - \mathcal{E}_Q(z) - S_Q(z) \quad (1)$$

where  $\Delta m_Q$  is the zero-point correction from the survey photometric system to the Vega system (or the AB system for surveys introduced later in this section that use the AB sys-

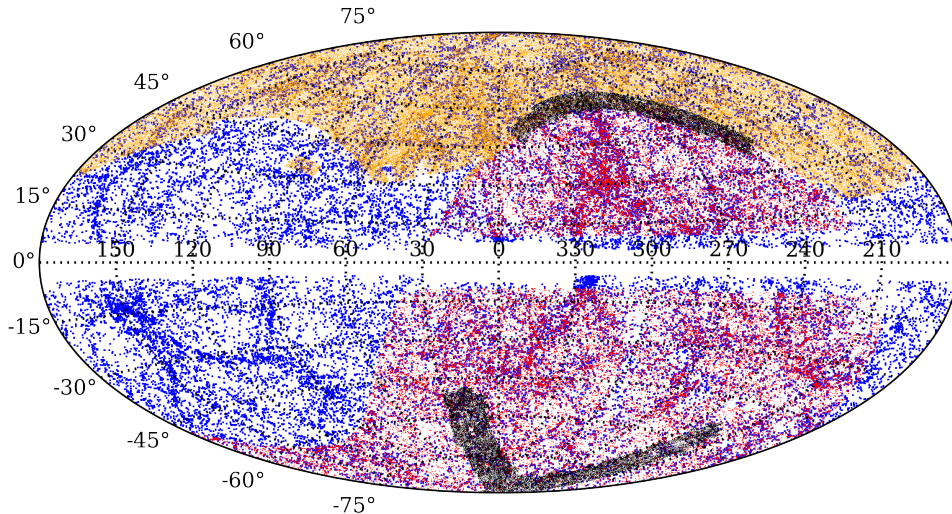


**Figure 2.** The galaxy distributions in Galactic coordinates (Aitoff projection) of the 2MRS (blue), 6dFGS (red), SDSS (orange), and 2dFGRS (black) samples.

**Table 1.** A summary of galaxy samples.

Sample	Sky Coverage (%)	Depth <sup>a</sup> ( $z$ )	Magnitude limit (mag)	No. of Galaxies <sup>b</sup>
2MRS	91%	0.08	$K_s \leq 11.75$	43,249 (44,310)
6dFGS	40%	0.11	$K_{s,tot} \leq 12.5$	62,987 (73,386)
SDSS	21%	0.2	$r \leq 17.77$	586,025 (600,458)
2dFGRS	3.3%	0.2	$b_J \leq 19.45$	180,967 (189,101)

**Notes.**

<sup>a</sup> Upper limit of redshift in CMB rest-frame.

<sup>b</sup> The numbers in parentheses are for the extended (the catalogs with ‘+’) catalogs.

tem), which is 0.017 for the 2MASS  $K_s$ -band filter (Cohen et al. 2003),  $DM(z)$  is the distance modulus at  $z$ ,  $\mathcal{K}_Q(z)$  and  $\mathcal{E}_Q(z)$  are the  $K$ - and evolution- corrections at redshift  $z$ , respectively, and  $\mathcal{S}_Q(z)$  corrects for the effect of decreasing aperture size within which flux is integrated with increasing redshift due to dimming of surface brightness. The term  $\mathcal{S}_Q(z)$  is not needed when using extrapolated total magnitudes. We follow Lavaux & Hudson (2011) to model  $\mathcal{K}_Q(z)$ ,  $\mathcal{E}_Q(z)$ , and  $\mathcal{S}_Q(z)$ , and correct the values of  $M_Q$  of individual galaxies to redshift  $z = 0.1$ . For nearby galaxies that have negative recession velocities in the CMB rest-frame (a total of 25 galaxies in the 2MRS catalog), we adopt distances from ‘EDD distances’ available at the Extragalactic Distance Database (EDD; Tully et al. 2009) to calculate the absolute magnitudes. These distances, however, are not used in identifying galaxy systems via the group finder, as our group finder works in redshift space. In the cases where we do not find matches from the EDD (a total of 5 galaxies in the 2MRS catalog), we assign the distances of their nearest neighbors that have EDD distances available. Later in §5

where we construct group catalogs, we estimate stellar mass using the mean relation between stellar mass and  $K_s$ -band luminosity from the simulation described in §2.5.

## 2.2 The 6dFGS catalog

Our second sample is selected from the 6dF Galaxy Survey (6dFGS; Jones et al. 2004, 2005). Specifically we use the 6dFGS Data Release 3 (6dFGS DR3; Jones et al. 2009), the final redshift release of the survey. As 2MRS, the 6dFGS is based mainly on the  $K_s$ -selected 2MASS, but is deeper, with a magnitude limit of  $K_{s,tot} = 12.65$  mag, where  $K_{s,tot}$  is the total magnitude from the 2MASS. Note that the magnitudes are corrected for foreground dust extinction, as mentioned above. As shown in McIntosh et al. (2006), these magnitudes are robust against uncertainties in surface brightness. The survey has a sky coverage of  $\sim 41\%$  in the southern hemisphere.

According to Jones et al. (2009), the final 6dFGS catalog contains 126,754 unique redshifts from their own obser-

vations, 563 redshifts from the SDSS, 5,210 redshifts from the 2dFGRS, and 9,042 redshifts from the ZCAT. For their own observations, the catalog contains only the spectra with quality parameters  $Q = 3$  and  $Q = 4$ , which are appropriate for scientific analysis according to Jones et al. (2009). Redshifts with  $Q = 3$  and  $Q = 4$  have typical uncertainties of 55 km/s and 45 km/s, respectively (see Jones et al. 2009, for details). However, the 6dFGS has poorer coverage in some regions, such as those toward the Large Magellanic Cloud (LMC) and the South Pole. This can affect the performance of our group finder. To reduce this effect we select a shallower sample, using the 2MASS Extended Source Catalog (2MASS XSC) with a flux limit of  $K_{s,tot} = 12.5$  mag as an input catalog. The 2MASS XSC with this flux limit contains 75,098 entries. For galaxies that have spectroscopic redshifts from the 6dFGS catalog, we assign the 6dF redshift. We also find redshifts for 1,533 galaxies from the 2M++ galaxy redshift catalogue (2M++; Lavaux & Hudson 2011), which are originally from the NED. For galaxies without spectroscopic redshifts available, we assign redshifts of their nearest neighbors or from the 2MPZ in the same way as for the 2MRS described above. Of all the 2MASS XSC galaxies, 62,929 have redshifts from the 6dFGS DR3, 1,533 redshifts from the 2M++, 3,354 redshifts from the nearest neighbor, and 7,282 redshifts from the 2MPZ. This, of course, corresponds to 100% redshift completeness. In the end, we will provide two separate catalogs: one constructed using only galaxies with spectroscopic redshifts, and the other using all galaxies, including the ones with nearest-neighbor and 2MPZ redshifts. For convenience, we refer to the 1st catalog as 6dFGS, and the 2nd catalog as 6dFGS+.

For our analysis, we correct all the radial velocities (redshifts) to the CMB rest-frame, as we did for the 2MRS, and we only use galaxies with corrected redshift  $z \leq 0.11$ . This leaves 62,987 and 73,386 galaxies in our final 6dFGS and 6dFGS+ samples, respectively. The redshift distribution and a summary of the final samples are given in Figure 1 and Table 1, respectively.

The absolute magnitudes of individual galaxies are again calculated using equation (1). The same  $K$ -,  $E$ -, and surface brightness corrections as those for the 2MRS are used to correct the  $K_s$ -band magnitudes to  $z = 0.1$ . For galaxies with negative recession velocity, we again use the EDD distances to compute their luminosities. We approximate stellar mass using the mean relation between stellar mass and  $K_s$ -band luminosity obtained from the simulation described in §2.5.

### 2.3 The SDSS catalog

Our third sample is selected from the Sloan Digital Sky Survey Data Release 13 (SDSS DR13; Albareti et al. 2016). DR13 is the first data release of the fourth phase of the Sloan Digital Sky Survey (SDSS-IV) and is built upon prior releases. It includes updated data for the SDSS Legacy Survey, which is a magnitude limited redshift survey completed in SDSS-II, as well as objects from the Baryon Oscillation Spectroscopic Survey (BOSS; Dawson et al. 2013), the selection of which barely overlaps with that of the legacy survey. The main part of the SDSS Legacy Survey was already released in DR7, and remained more or less steady through DR12. Significant changes were made to photometric cal-

ibration in the DR13, including updated zero points and flat-fields in the  $g$ ,  $r$ ,  $i$ , and  $z$  bands from the hypercalibration procedure of Finkbeiner et al. (2016). These affect all photometric quantities of the galaxies in the Legacy Survey. In addition to the updated photometry calibration, another significant improvement in DR13 relative to, for example, DR7 is that some of the fiber-collision galaxies in DR7 have their redshifts measured in DR13. The SDSS spectrograph used for the Legacy Survey did not allow two fibers to be positioned within  $55''$ , and so no spectroscopic measurement was available for galaxies that have close neighbors within the fiber separation, the so-called ‘fiber-collision’ galaxies. Many of the ‘fiber-collision’ galaxies ( $\sim 60\%$ , e.g. Guo et al. 2015) have been measured spectroscopically in the later data releases through DR13. The Legacy Survey covers approximately  $\sim 23\%$  of the sky, and is complete to an extinction-corrected Petrosian magnitude of 17.77 mag in the  $r$ -band.

From the full photometric catalog of DR13, we select all objects that are in the Legacy Survey region and identified as galaxies (type = 3) brighter than the  $r$ -band magnitude limit of 17.77. We take the photometric quantities only from the primary observation in the cases where an object was observed multiple times (mode = 1). We also get rid of galaxies in the Southern Galactic Cap, as its narrow angular boundary makes our group finder unreliable for many systems close to the boundary. Note that these selections may include some of the BOSS galaxies that pass the selection criteria. The selections leave a total of 638,191 entries, of which 16,251 galaxies do not have redshifts for reasons such as fiber-collisions, broken or unplugged fibers, bad spectra, or poor fit to models. Of the 621,940 galaxies that have redshifts, 20,780 ( $\sim 3.3\%$ ) are BOSS galaxies in the Legacy region.

For the 16,251 galaxies without SDSS redshifts, we find redshifts from other sources: the 2dFGRS, 6dFGS, the Korea Institute for Advanced Study Value-Added Galaxy Catalog (KIAS VAGC; Choi et al. 2010), a complementary galaxy sample in the LAMOST Survey (Luo et al. 2015; Shen et al. 2016), the nearest neighbors, or the 2MPZ, to achieve 100% redshift completeness. For galaxies that have redshifts available from more than one sources, preferences are given in the order given above, i.e. from 2dFGRS to 2MPZ. As a result, 294, 29, 168, 227, 13,548, and 1,985 additional redshifts are obtained from 2dFGRS, 6dFGS, KIAS VAGC, LAMOST, the nearest neighbors, and 2MPZ, respectively. In the following, we will construct two different kinds of group catalogs from the SDSS data, one using only galaxies that have spectroscopic redshifts, and the other using all galaxies including the ones with estimated redshifts from nearest neighbors and from 2MPZ. For brevity, we refer to the 1st catalog as the SDSS and the 2nd as the SDSS+. We convert all the recession velocities (redshifts) to the CMB rest-frame, and restrict our samples to  $z \leq 0.2$ . This leaves a total of 586,025 and 600,458 galaxies as our final SDSS and SDSS+ samples, respectively.

We compute the absolute magnitudes in the  $r$ -band of the sample according to equation (1), using the WMAP9 cosmology, with  $K$ - and evolution- corrections to  $z = 0.1$  following Poggianti (1997). We also calculate the  $(g - r)$  color, corrected to  $z = 0.1$ , for each galaxy. From the DR13 photometric catalog, we adopt the *cmodel* magnitude to calculate the flux, and the model magnitudes to compute the

color, following the recommendations of the SDSS team. The zero-point offset between the DR13 magnitude and the AB magnitude is practically zero for  $g$ - and  $r$ - bands within the error of 0.01 mag. Galaxies with colors outside the  $3\sigma$  of the color distribution at a given luminosity are assigned the median color. For galaxies with negative redshifts, their luminosities are obtained from their EDD distances. Finally, we estimate the stellar masses of individual galaxies from their  $r$ -band absolute magnitudes and  $(g-r)$  colors, following the formula of Bell et al. (2003):

$$\log M_* = -0.306 + 1.097(g-r) + 0.4(4.67 - M_r), \quad (2)$$

where 4.67 is the absolute magnitude of the Sun in the  $r$ -band.

## 2.4 The 2dFGRS catalog

Finally, we also select a sample from the 2dF Galaxy Redshift Survey (2dFGRS; Colless et al. 2001). The 2dFGRS provides redshifts for about 250,000 galaxies, measured with the Two-degree Field (2dF) multifibre spectrograph on the Anglo-Australian Telescope, down to a magnitude limit of  $b_J = 19.45$  after Galactic extinction correction. The survey consists of two strips in the northern and southern Galactic hemispheres (the northern and southern Galactic caps, respectively), and 99 ‘random’ fields of  $2^\circ$  each over and around the southern Galactic cap. The full survey covers about  $2,000\text{deg}^2$  with a median redshift of  $z \sim 0.11$ . Because the random fields are not contiguous and our group finder can be affected severely at the edges of these field, we use only the two Galactic caps for our purpose. The final sky coverage of our sample is about 3.5%.

The quality of a spectrum is characterized by a quality parameter,  $Q = 1 - 5$ , with a higher value of  $Q$  indicating higher quality. From the final release spectroscopic catalog, we use only galaxies with  $Q \geq 3$ , for which the redshifts are 98.4 per cent reliable, with a typical uncertainty of 85 km/s (Colless et al. 2001). Of all the 245,591 galaxies from the 2dFGRS catalog, 12,340 systems do not have spectroscopic redshifts from the survey. For these galaxies, we find matches and assign redshifts from the SDSS DR13, the 6dFGS, the nearest neighbors, and the 2MPZ. In the cases where a galaxy has redshifts from more than one of these sources, the priority is given, in the order of decreasing priority, to the SDSS, the 6dFGS, the nearest neighbor redshift, and the 2MPZ. As a result, we have 233,251 redshifts from the 2dFGRS, 322 from the SDSS, 43 from the 6dFGS, 11,852 from the nearest neighbors, and 123 from the 2MPZ. Again, we will provide two catalogs, one using only galaxies with spectroscopic redshifts, and the other using all galaxies. We refer to these two catalogs as the 2dFGRS and 2dFGRS+ samples, respectively.

Redshifts are corrected to the CMB rest-frame, and we limit our sample to  $z \leq 0.2$ . The final samples contain 180,967 and 189,101 galaxies for the 2dFGRS and 2dFGRS+, respectively. When selecting galaxy groups from these samples, we adopt the survey masks provided in the 2dFGRS website †. For reference, the redshift distribution of 2dFGRS is shown in Figure 1.

We use equation (1) to convert the observed apparent magnitudes to absolute magnitudes, assuming WMAP9 cosmology. To do this, we first make  $K$ - and  $E$ - corrections to  $z = 0.1$  following the method given in Poggianti (1997). The stellar masses of individual galaxies are obtained from their  $b_J$ -band absolute magnitudes and  $b_J - R$  colors using the approximation of Bell et al. (2003):

$$\log M_* = -0.976 + 1.111(b_J - R) + 0.4(5.48 - M_{b_J}), \quad (3)$$

where 5.48 is the absolute magnitude of the Sun in the  $b_J$ -band. For a small number of galaxies that have colors outside the  $3\sigma$  range of the  $b_J - R$  distribution, and for a total of 276 galaxies without the  $R$ -band photometry, each of them has been assigned a  $(b_J - R)$  color that is equal to the median value given by the galaxies which have  $b_J$  luminosities similar to the galaxy in question and have  $b_J - R$  colors. Here again, the EDD distances have been used to convert the observed flux to the luminosity for galaxies with negative redshifts.

## 2.5 Mock samples used to test methods

The quality of the group samples to be constructed depends on the performance of the group finder used to identify the groups from the observational data. To test the performance of our group finder (to be described in §3), we use mock samples constructed from a hydrodynamical simulation of galaxy formation, where information about dark matter halos and their galaxy memberships are all known.

The hydrodynamical simulation used here is the Evolution and Assembly of GaLaxies and their Environments (EAGLE; Schaye et al. 2015; Crain et al. 2015; McAlpine et al. 2015). EAGLE follows the evolution of gas, stars, dark matter, and massive black holes in a cosmological context, implementing physical models for gas cooling, star formation, stellar and AGN feedback. Sub-grid processes, in particular feedback processes, are modeled with simple parametric forms, with model parameters tuned to match observations, such as the stellar mass function and stellar mass - black hole mass relation at  $z \sim 0$ , as detailed in Crain et al. (2015). The simulation starts from  $z = 127$  and adopts the *Planck* cosmology with  $(\Omega_m, \Omega_\Lambda, h) = (0.307, 0.693, 0.678)$  (Planck 2014). This cosmological model is not exactly the same as the WMAP9 cosmology we adopt in this paper. However, since the purpose here is to test our group finder and halo mass proxies (see below), this difference in cosmology should not be a concern, as long as the analysis is done in a self-consistent way. EAGLE provides a set of simulations assuming different sets of model parameters and different box sizes. Here we use the simulation with the largest box size of  $100\text{Mpc}^3$ , their fiducial simulation. The simulation contains about 11,500 dark matter halos with masses above  $10^{11}M_\odot$ , and  $\sim 10,000$  galaxies with masses comparable to or above that of the Milky Way. EAGLE adopted the Chabrier (2003) IMF and the spectral synthesis model of Bruzual & Charlot (2003) to get luminosities and stellar masses of individual galaxies from their star formation histories, and these are used in our analysis as well. A few galaxies are found to have extremely low halo masses for their stellar masses. These extreme outliers are excluded from our analysis.

We construct realistic mock catalogs of galaxies from

† <http://www.2dfgrs.net/>

EAGLE. Since the original simulation box, 100 Mpc, is smaller than the volumes of our samples, we stack the duplicates of the original box side by side as many times as is required to cover the volume of the sample in question. A location is chosen for the observer in the stack, and apparent magnitudes of individual galaxies are calculated from their luminosities and their distances to the observer. The same sample selections as those for the observational samples, as detailed earlier in this section, are applied to construct the mock samples. Specifically, we choose galaxies in the simulation box that are in the same sky regions as the observational samples, as well as apply the apparent magnitude and redshift limits of each survey to eliminate faint galaxies from the mock samples. Finally, we also apply the same masks, if any, as provided for the observational samples by each survey. Since all the galaxies in the simulation are linked to dark matter halos, we can use these mock catalogs to quantify the accuracy of our methods.

As an independent check, we have also constructed mock samples using an empirical model of galaxy formation. The details of these mock samples are given in Appendix A.

### 3 THE HALO-BASED GROUP FINDER

#### 3.1 The basic algorithm

The method adopted here is similar to the ‘halo-based’ group finder developed by Yang et al. (2005) (Y05 hereafter). This group finder makes use of physical properties of dark matter halos expected from the current cold dark matter (CDM) cosmogony, such as halo mass, virial radius and velocity dispersion, in assigning galaxies into groups. The group finder has been tested extensively using mock galaxies, and is found to be more effective than the traditional Friends-of-Friends (FoF) algorithm in grouping galaxies according to common halos, and particularly in dealing with poor groups associated with small halos. This allows the identification of systems over a wide range of masses. However, in the original group finder of Y05, halo masses assigned to galaxy groups are based on the ranking order of the total luminosity of member galaxies (or the sum of the luminosities of member galaxies above a certain luminosity limit). It becomes inaccurate for groups that contain only a small number of members, and is not appropriate for shallow surveys where a large number of the identified groups contain only one or a small number of relatively bright galaxies. In order to overcome this limitation, we make some modifications to the group finder of Y05, in particular in the assignments of masses to galaxy groups. Specifically, for systems containing more than one member galaxy, we adopt a modified version of the ‘GAP’ model developed by Lu et al. (2016). For systems containing only one member, we use halo mass proxies that are calibrated by realistic mock catalogs. As we will show below, these modifications not only provide more accurate halo mass estimates, but also allow us to reach to systems with lower halo masses in a uniform way. The detailed steps of the group finder are as followings:

- Step 1. *Assign preliminary halo mass to every galaxy.*

While the group finder of Y05 starts by linking galaxies using the FoF algorithm with a small linking length to

identify preliminary group centers, we start by treating all galaxies as isolated galaxies associated with distinct tentative dark matter halos with preliminary halo masses computed according to the halo mass proxies described in §3.2. We have checked that this leads to no significant differences in membership, mass, and the number of final groups in comparison to that of Y05.

- Step 2. *Membership assignment using halo properties.*

For all groups identified at each iteration, we compute the size and the line-of-sight velocity dispersion, which are used to determine which galaxies should be assigned to a certain group,

$$\begin{aligned} \frac{r_{180}}{\text{Mpc}} &= 1.33 h^{-1} \left( \frac{M_h}{10^{14} h^{-1} M_\odot} \right)^{1/3} (1 + z_{\text{group}})^{-1} \\ \frac{\sigma}{\text{km s}^{-1}} &= 418 \left( \frac{M_h}{10^{14} h^{-1} M_\odot} \right)^{0.3367}, \end{aligned} \quad (4)$$

where  $z_{\text{group}}$  is the redshift of the group in question, and  $r_{180}$  is the radius of the halo, within which the mean mass density is 180 times the mean density of the universe at the given redshift. The numbers used are appropriate for the WMAP9 cosmology (e.g. Lu et al. 2016). Next, we assume that the phase-space distribution of galaxies in dark matter halos follows that of dark matter particles and that the group center is the same as the halo center. The number density contrast of galaxies at the redshift of  $z_{\text{group}}$  can then be expressed as

$$P_M(R, \Delta z) = \frac{H_0}{c} \frac{\Sigma(R)}{\bar{\rho}} p(\Delta z) \quad (5)$$

where  $R$  is the projected distance,  $c$  is the speed of light,  $\bar{\rho}$  is the mean density of the Universe,  $\Sigma(R)$  is the surface density, and  $\Delta z = z - z_{\text{group}}$ . We assume that the redshift distribution of galaxies within a halo,  $p(\Delta z)$ , has the Gaussian form,

$$p(\Delta z) = \frac{c}{\sqrt{2\pi}\sigma(1 + z_{\text{group}})} \exp\left( \frac{-c^2 \Delta z^2}{2\sigma^2(1 + z_{\text{group}})^2} \right) \quad (6)$$

where  $\sigma$  is the line-of-sight velocity dispersion. Furthermore, halos are assumed to follow a spherical NFW density profile, so that the surface density  $\Sigma(R)$  can be written as

$$\Sigma(R) = 2r_s \bar{\delta} \bar{\rho} f(R/r_s) \quad (7)$$

where  $r_s$  is the scale radius, and

$$f(x) = \begin{cases} \frac{1}{x^2-1} \left[ 1 - \frac{\ln \frac{1+\sqrt{1-x^2}}{x}}{\sqrt{1-x^2}} \right], & \text{if } x < 1 \\ \frac{1}{3}, & \text{if } x = 1 \\ \frac{1}{x^2-1} \left[ 1 - \frac{\text{atan} \frac{\sqrt{x^2-1}}{\sqrt{x^2-1}}}{\sqrt{x^2-1}} \right], & \text{if } x > 1 \end{cases}$$

$$\bar{\delta} = \frac{180}{3} \frac{c_{180}^3}{\ln(1 + c_{180}) - c_{180}/(1 + c_{180})} \quad (8)$$

with the concentration,  $c_{180} = r_{180}/r_s$ , given by the model of Zhao et al. (2009). Finally, we calculate  $P_M(R, \Delta z)$  for each of all the galaxy-group pairs. If the value of  $P_M$  is above a certain background value,  $P_B$ , an association between the galaxy and the group is assumed. If a galaxy is

associated with more than one group according to this criterion, the galaxy is assigned to the group with the largest  $P_M(R, \Delta z)$ . As demonstrated in Y05 using realistic mock samples, a compromise between the completeness and contamination can be achieved with  $P_B \sim 10$ , and the performance of the group finder is not very sensitive to the exact value of  $P_B$ . Note that  $P_B \sim 10$  is also in agreement with theoretical expectations for dark matter halos (see the discussion in section 3.2 of Y05 for details). We therefore adopt  $P_B = 10$  throughout this paper.

After the membership of a group is determined, we define the stellar mass-weighted center of member galaxies as the group center, if stellar masses are available. Otherwise, we use luminosity-weighted center as the group center.

- Step 3. *Rank groups according to halo mass proxies.*

As described in §3.2.1 and §3.2.2, in the beginning of each iteration, tentative halo masses are assigned to groups identified in the previous step by ranking groups according to a mass proxy. In short, for tentative groups containing only one member galaxy in the previous step, we use the galaxy stellar mass (luminosity) - halo mass relation obtained from a hydrodynamical simulation to assign the preliminary halo mass, as described in §3.2.2. For tentative groups that contain more than one member at a given iteration, we use the ‘GAP correction’ method of Lu et al. (2016), modified with our own re-calibrations (see below).

- Step 4. *Group mass update and iteration.*

To assign masses to groups, we use abundance matching between the mass function of the preliminary groups and an adopted theoretical halo mass function. A new halo mass,  $M_{\text{halo}}$ , is assigned to a group to replace the preliminary group mass,  $M_{\text{pre}}$ , according to

$$N(> M_{\text{halo}}) = N(> M_{\text{pre}})$$

where  $N$  is the cumulative number density of groups (halos) more massive than  $M_{\text{pre}}$  ( $M_{\text{halo}}$ ). We use the theoretical halo mass function of Sheth et al. (2001) for this. Note that for flux-limited samples, halos of a given mass are complete only to a certain redshift. The abundance matching used to assign halo mass is applied only for groups in samples that are complete (see §4.2). For groups residing in volumes within which the samples are not complete, we use the mean relation between the halo mass and the mass proxy from the last iteration to assign halo masses to them. Once group masses are updated, we iterate Steps 2 through 4 until convergence in group membership is achieved.

### 3.2 Halo mass proxies of galaxy groups

As mentioned in the previous section, our group finder relies on the reliability of the halo mass model for groups. Here we test different halo mass proxies by comparing their predictions with the results obtained from the hydrodynamical simulation. We have also made similar tests using a mock sample of galaxies constructed by applying the empirical model of Lu et al. (2015) to the simulated halos. The results obtained from the empirical model are very similar to

those obtained from the hydrodynamical simulation, and are presented in Appendix A.

#### 3.2.1 Halo mass proxies for groups containing more than one galaxy

In the original paper presenting the halo-based group finder, Y05 uses the sum of the luminosities of member galaxies down to some luminosity limit as a proxy of group masses. However, this proxy may not be appropriate for a shallow galaxy survey where many groups have only a small number of members. Because of this, Lu et al. (2016) (L16 hereafter) suggested the use of a combination of the luminosity/stellar mass of the central galaxies, and the luminosity/stellar mass GAP (the difference in luminosity/stellar mass between the central galaxy and the  $n$ -th brightest galaxy) as a group mass proxy. Based on mock galaxy samples, L16 came up with the following model for the halo mass,

$$\log M_h(L_c, L_{\text{gap}}) = \log M_h(L_c) + \Delta \log M_h(L_c, L_{\text{gap}}) \quad (9)$$

where  $L_c$  is the luminosity of the central galaxy,  $M_h(L_c)$  is the mean halo mass at a given  $L_c$ , and  $L_{\text{gap}} = L_c/L_n$  with  $L_n$  the luminosity of the  $n$ -th brightest satellite. The masses and luminosities here are in units of  $M_\odot/h$  and  $L_\odot/h^2$ , respectively. Using mock samples constructed for the 2MRS, L16 found that their group masses are consistent with true halo masses obtained from the simulation used in their mock samples, and the best result is achieved with  $n = 4$ . For groups with less than four satellites, L16 used the faintest satellite in a group for the GAP correction. The basic motivation behind the GAP correction is that groups of the same central galaxy luminosity but with more contribution from satellites should possess more massive halos.

Here we adopt the same idea of the GAP correction, but use our own functional form for  $\Delta \log M_h(L_c, L_{\text{gap}})$ :

$$\Delta \log M_h(L_c, L_{\text{gap}}) = \alpha(L_{\text{gap}}) \times (\log L_c - \beta)^\gamma + \delta(L_{\text{gap}})$$

with

$$\begin{aligned} \alpha(L_{\text{gap}}) &= \alpha_1 + \alpha_2 \log(L_{\text{gap}}) \\ \delta(L_{\text{gap}}) &= \delta_1 + \delta_2 \log(L_{\text{gap}}) + \delta_3 [\log(L_{\text{gap}})]^2 \end{aligned} \quad (10)$$

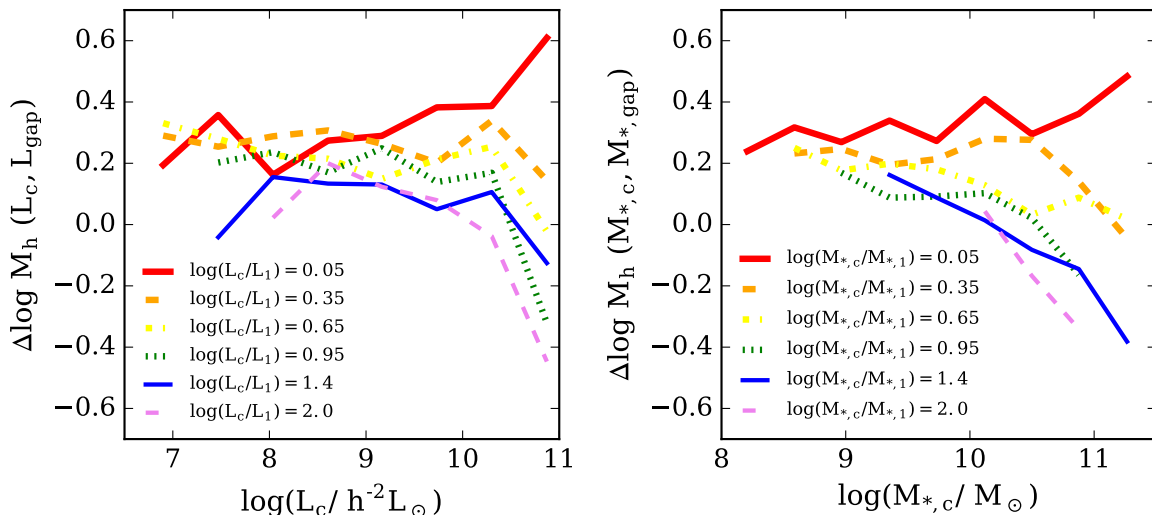
where the free parameters  $\alpha_1$ ,  $\alpha_2$ ,  $\beta$ ,  $\gamma$ ,  $\delta_1$ ,  $\delta_2$ , and  $\delta_3$  are constants, and the masses and luminosities are again in solar units. We use mock catalogs constructed from EAGLE to calibrate these free parameters. For example, from the 2MRS mock catalog we obtain  $(\alpha_1, \alpha_2, \beta, \gamma, \delta_1, \delta_2, \delta_3) = (-2.3 \times 10^{-5}, -1.1 \times 10^{-6}, 6.6, 5.1, 0.28, 0.13, 0.035)$  for  $L_{\text{gap}} = L_c/L_2$ . The values of these parameters for other cases are given in Table 2.

As shown later in this section, the use of stellar masses gives better halo proxies than the use of luminosities. Thus, halo masses based on stellar masses are preferred to those based on luminosities whenever stellar masses are available. The halo mass proxy using stellar mass is modeled in the same way as that given above, except with  $L_c$  and  $L_{\text{gap}}$  replaced by  $M_{*,c}$  and  $M_{*,\text{gap}}$ , respectively. Figure 3 shows the relations given by equations (9) and (10) using galaxy luminosities or galaxy stellar masses.



**Table 2.** The best-fit parameters for the GAP correction from the EAGLE.

Sample	$\alpha_1$ ( $\times 10^5$ )	$\alpha_2$ ( $\times 10^6$ )	$\beta$	$\gamma$	$\delta_1$	$\delta_2$	$\delta_3$
2MRS	-2.3	-1.1	6.6	5.1	0.28	0.13	0.035
6dFGS	-1.1	-3.9	4.8	6.1	0.13	-0.15	0.037
SDSS	-3.6	-6.0	5.3	5.2	0.11	-0.039	0.0014
2dFGRS	-3.6	-5.9	5.5	5.7	0.12	-0.046	0.0035

**Figure 3.** Dependence of halo mass on the luminosity or stellar mass of the central galaxy and the GAP parameter (defined to be the difference in luminosity or stellar mass between the central galaxy and the  $n$ -th brightest satellite; see text for detailed definition) as given by EAGLE. The left panel is the result based on the  $K$ -band luminosity, while the right panel shows result based on stellar mass. For clarity, only the GAP correction using the brightest satellite (i.e.  $n = 1$ ) is shown.

### 3.2.2 Halo mass proxies for groups containing one galaxy

Next we consider systems that contain only one member galaxy. Here we present the best proxy for such systems for each catalog based on tests with a number of proxies. Note that the GAP correction from the previous section is not applicable for isolated galaxies, as by definition there is no observed satellite in systems containing only one member. In L16, it was assumed that each isolated galaxy has, with 50% chance, one potential satellite galaxy with  $K_s = 11.75$ , which is the magnitude limit of 2MRS catalog. The average of the corresponding GAP-corrected group mass and  $M_h(L_c)$  were used as the halo mass proxy in L16, if the GAP-correction  $\Delta \log M_h$  is larger than 0.5. Such a prescription sometimes leads to too high or too low a halo mass for a given  $L_c$  according to our test with the mock samples used here. Because of this, here we attempt to revise the proxy so that it is more reliable for groups with only one member.

#### 3.2.2.1 Proxy- $L$ : Galaxy luminosity

Our first halo mass proxy is based on the luminosities of galaxies. To do this, we first obtain the luminosity - halo

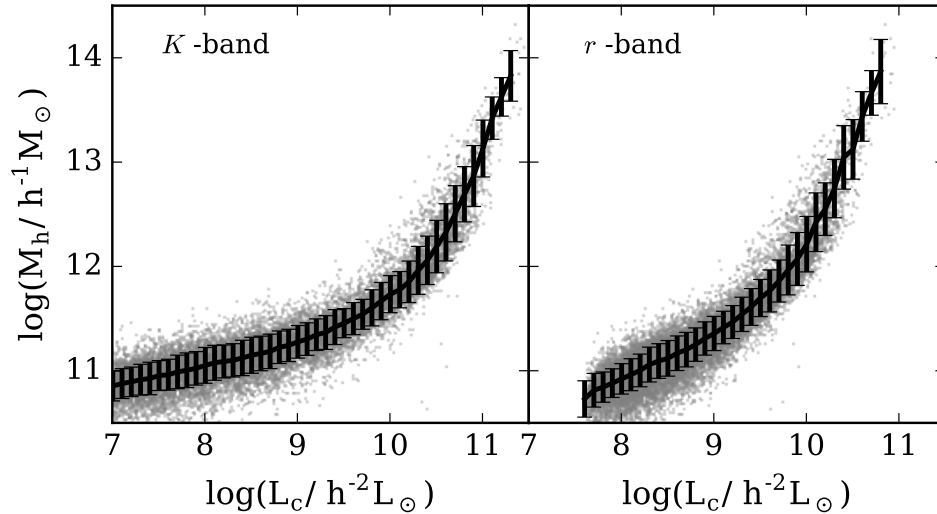
mass relation of central galaxies from EAGLE. Figure 4 shows such relations in the  $K$ -band and  $r$ -band. The distribution of the halo masses at a given luminosity is roughly log-normal. In the  $K$ -band, which will be used for both 2MRS and 6dFGS, the mean relation can be well described by

$$\log M_h = 10.789 + 2.109 \times 10^{-4} \exp(\log L_c / 1.184) \quad (11)$$

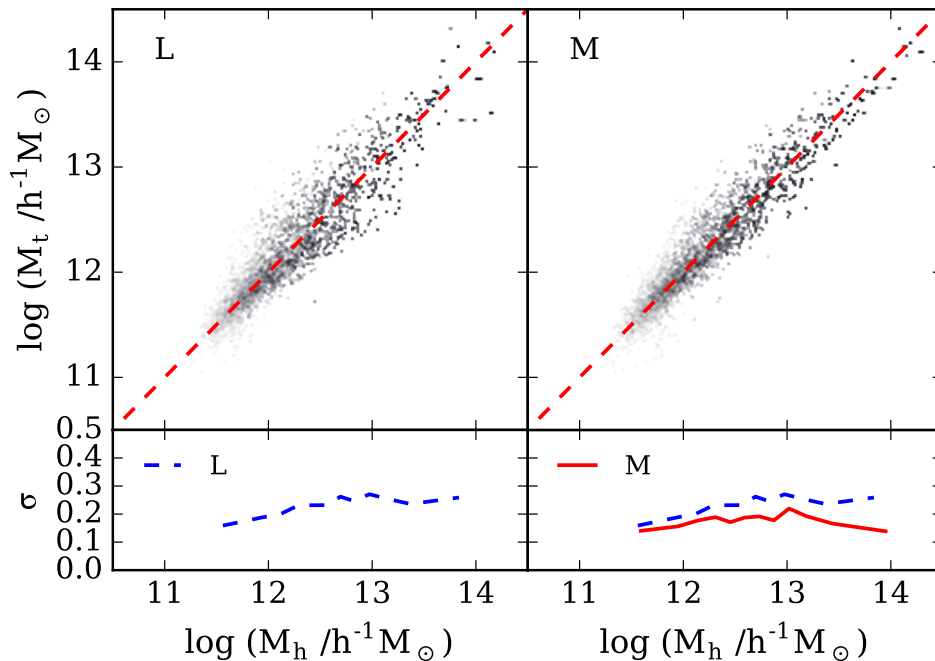
and the typical width is about 0.2 dex. The units of  $M_h$  and  $L_c$  are in  $M_\odot/h$  and  $L_\odot/h^2$ , respectively. In the  $r$ -band, which will be used for SDSS and 2dFGRS, the mean relation is given by

$$\log M_h = 10.595 + 4.370 \times 10^{-4} \exp(\log L_c / 1.214) \quad (12)$$

and the width of the log-normal distribution is about 0.22 dex. We assign the mean halo mass at a given luminosity as the tentative halo mass to each galaxy. We also tested generating a random mass at given luminosity around the mean halo mass and using it as the mass proxy, and found that the resulting scatter between the true halo mass and final halo mass from the group finder is larger by  $\sim 0.1$  dex than that given by using the mean relation.



**Figure 4.** The relation between the  $K$ -band (left) and the  $r$ -band (right) luminosity of central galaxies and the halo mass, as obtained from the EAGLE simulation. The gray points are individual systems, while the black line and bars show the median and scatter of the relation, respectively.



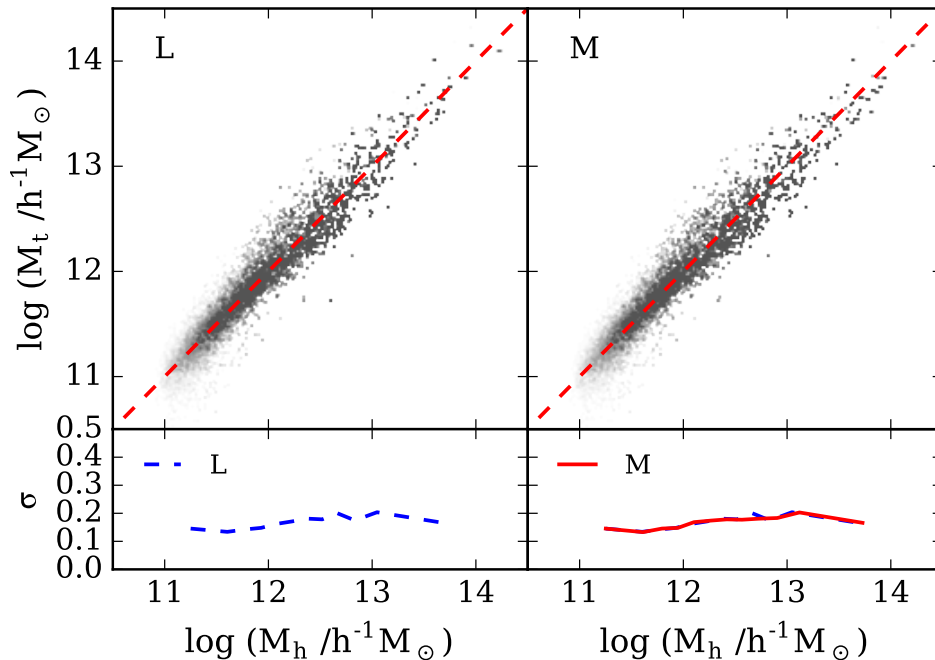
**Figure 5.** The correlations of the halo masses given by a mass proxy for groups containing a single member galaxy (horizontal axis) with the true halo mass (vertical axis), obtained from the 2MRS mock sample constructed with the EAGLE simulation. The results shown use proxies based on the  $K$ -band luminosity (L; left), and stellar mass (M; right). The red straight line in each big panel shows a perfect correlation, while the curves in the smaller panels show the scatter in the correlation.

Figure 5 compares the group masses given by the group finder with true halo mass from EAGLE for the 2MRS mock sample. The overall agreement between true mass and group mass using this proxy is found to have scatter of 0.2 – 0.25 dex. Note that Figure 5 only includes isolated galaxies, which are expected to have larger scatter than

groups of more than one member for which the GAP correction will be used.

### 3.2.2.2 Proxy-M: Galaxy stellar mass

We also test a halo mass proxy based on stellar mass of the central galaxy. To do this, we use the mean relation between



**Figure 6.** The same comparison as in Figure 5 but here for the SDSS mock sample.

the halo mass and stellar mass of isolated galaxies from EAGLE to assign preliminary halo mass. Figure 5 shows the comparison of the resulting final group mass with true halo mass. It is clear that the scatter in the group mass is significantly reduced, by  $\sim 0.05$  dex or more, relative to Proxy-L, suggesting that stellar mass is a better halo mass proxy for isolated galaxies. In real observations, however, stellar mass estimates introduce additional uncertainties. Thus we provide catalogs based on both Proxy-L and Proxy-M in §5, where we construct and present our group catalogs.

Figure 6 shows the same comparisons between the true and estimated halo masses for the SDSS mock sample. The two mass proxies, Proxy-L and Proxy-M are used in the same way as described above for the 2MRS mock, except that the parameters in the mass models are obtained for the SDSS  $r$  magnitude. We see that for the SDSS mock catalog, the two mass proxies give very similar scatter in the halo mass,  $\sim 0.15 - 0.2$  dex. This is different from 2MRS, for which Proxy-M appears to be significantly more accurate than Proxy-L. This may be due to the fact that isolated galaxies in the SDSS mock are dominated by low-mass galaxies (because of its fainter magnitude limit) for which the galaxy color does not depend systematically on halo mass. We also found the same level of scatter, with perhaps a slight increase at the massive end, in tests based on the mock samples constructed from the empirical model, where uncertainties such as that in the stellar mass measurements, are taken into account.

### 3.2.2.3 Other proxies tested

We have tested a number of other quantities available from the EAGLE such as velocity dispersion and metallicity of galaxies, as well as halo formation time and local density of galaxies. While some of these quantities are also found

to be strongly correlated with halo mass according to the simulations, we found that halo mass proxies based on these quantities are not as accurate as those given by stellar mass and luminosity. We have also tested using combinations of stellar mass/luminosity and one of these additional quantities as halo mass proxies and found that none of them makes significant improvement in the halo mass estimate, at least according to the simulation we use here. Note also that these additional quantities are usually not available from actual observations, making them less useful in practice.

Motivated by L16 who used a ‘GAP limit’ as a second parameter in the halo mass proxy for isolated galaxies, we have also made tests with the use of some measurements of the ‘GAP limit’. The GAP limit, as defined in L16, is the GAP correction described in the previous section but using  $G_{\text{gap,lim}} = L_c/L_{\text{lim}}$  instead of  $G_{\text{gap}} = L_c/L_n$ , where  $L_{\text{lim}}$  is the luminosity that corresponds to the observational magnitude limit at the redshift of the galaxy in question. Thus, an isolated galaxy with smaller  $G_{\text{gap,lim}}$  should have, on average, a more massive satellite that is not observed due to the magnitude limit. The ‘GAP limit’ is an attempt to take such an effect into account. However, our test showed that using ‘GAP limit’ does not lead to further improvement in the final halo mass.

Given all these test results, we use the stellar mass when it is available, and use luminosity otherwise, as the halo mass proxy for isolated galaxies. However, given the observational uncertainties in stellar mass estimates, we will provide two catalogs for each data set: a catalog constructed based on Proxy-L and a catalog based on Proxy-M.

#### 4 TESTING THE GROUP FINDER WITH MOCK SAMPLES

Before we apply the group finder to observational samples, we test its performances by applying it to realistic mock samples described in §2.5, and analyzing the accuracy of group masses, and the completeness, contamination and purity of group memberships that are expected from each of the observational samples.

##### 4.1 Applying the group finder to the mock samples

As we have shown, stellar mass is theoretically a better proxy of group mass than luminosity (see §3) but only when observational uncertainties in stellar mass estimate are negligible. Therefore, we present catalogs that use both luminosity and stellar mass as mass proxies. We use the GAP correction in luminosity (or stellar mass) for groups with more than one member, and Proxy-L (or Proxy-M) for isolated galaxies.

##### 4.2 Group mass estimates

In the end of each iteration of the group finder, we finalize group masses using abundance matching. The abundance matching is applied only to volumes within which groups of a given mass are complete. As the surveys and the mock samples are flux-limited, halos of a given mass are only complete to a certain redshift. Figure 7 shows the number of halos as a function of redshift for each mock sample from the simulation. As one can see, in each case the number of groups first follows well the expectation of a constant density indicated by the dashed curve in each panel, and starts to go below the expectation at some redshift as incompleteness becomes severe. We can therefore define a limiting redshift, within which the group sample in question is approximately complete. The limiting redshift,  $z_{\text{lim}}$ , is indicated as the dot vertical line in each panel, and Figure 8 shows the value of  $z_{\text{lim}}$  as a function of halo/group mass for the four mock samples corresponding to the four observational samples. These relations can all be well described by a power law,  $(1+z_{\text{lim}}) \propto M_{\text{h}}^{\zeta}$ , as shown in Figure 8. The limiting redshifts obtained in this way are used to define complete samples for abundance matching. For groups that are outside the limiting redshift, we use the mean relation between halo mass and the mass proxy to assign halo masses to them.

Figure 9 compares the true halo masses from the simulation with the final group masses obtained by our group finder using the  $K_s$ -band ( $r$ -band, for the SDSS and 2dFGRS) luminosity as the mass proxy. It is clear that the group finder performs quite well in assigning correct masses to groups over the whole range of halo mass for various samples. No significant bias is seen in the assigned mass for any of the samples. The horizontal stretching of the data points appearing at the massive end is due to the stacking of the simulation box and the small number of massive halos in the original simulation box. The true halo masses are exactly the same for some of the halos that are the duplicates of the same halo in the original simulation, but the group masses assigned to them can be different because they are located at different redshifts in the mock sample. For a given true

mass, the typical scatter in the assigned mass is  $\sim 0.2$  dex. The scatter is larger for the 2MRS and 6dFGS mock samples, reflecting the less tight  $K_s$ -luminosity vs. halo-mass relation than the  $r$ -luminosity vs. halo-mass relation in the simulation. Table 3 compares the total number of groups (halos) and the number of groups (halos) of given richness between the mock group catalogs and the original simulation.

Figure 10 shows the same comparison of halo mass but obtained using stellar mass as the mass proxy for all surveys. It is seen that, unlike in Figure 9, the scatter in halo mass is almost identical for all surveys, and that stellar mass performs as a better mass proxy than the  $K_s$ -band luminosity by  $\sim 0.05$  dex or more, as seen earlier in Figure 5, while the  $r$ -band luminosity is an as good proxy as the stellar mass for the deeper surveys.

##### 4.3 Completeness, contamination, and purity

In addition to group masses, comparisons are also made between the membership assignment by the group finder and the true membership given by the simulation. To do this, we first assume that each mock group identified corresponds to the simulation halo that is associated with the brightest member of the mock group. As a quantitative assessment of the membership assignment, we follow Yang et al. (2007) and define the following quantities,

- Completeness:  $f_c \equiv N_s/N_t$ ;
- Contamination:  $f_i \equiv N_i/N_t$ ;
- Purity:  $f_p \equiv N_t/N_g$

where  $N_t$  is the total number of member galaxies of each halo from the simulation,  $N_s$  is the number of member galaxies of the corresponding mock group that are true members of the simulation halo (thus  $N_s \leq N_t$ ),  $N_i$  is the number of member galaxies of the mock group that are not true members of the simulation halo, and  $N_g = N_i + N_s$  is the total number of members of the mock group. For a perfect group finder,  $N_s = N_t = N_g$  and  $N_i = 0$ , and so  $f_c = f_p = 1$  and  $f_i = 0$ .

Figure 11 shows the completeness, contamination, and purity for the mock groups of different masses. The 2MRS and 6dFGS mock samples appear to have better membership assignments than the deeper SDSS and 2dFGRS mock samples. This happens because, in the two shallower samples, larger fractions of groups have a single member galaxy, which by definition have perfect completeness and zero contamination. For the 2MRS and 6dFGS mocks,  $\sim 90\%$  of all groups have completeness  $\sim 100\%$ , being lower for more massive halos. For the SDSS and 2dFGRS, about 85% (95%) of the groups have completeness  $\geq 95\%$  ( $\sim 70\%$ ). On the other hand, about 95% and 90% of the groups have zero contamination for the shallower two and deeper two surveys, respectively. Overall 80 – 90% of the groups have purity between 0.95 and 1.05, indicating that there is only a 5% difference in the total number of members between the true and selected memberships. We also check the global completeness of the identified groups as a function of redshift, and the results are shown in Figure 12. As expected, it declines beyond the redshift to which halos of a given mass is complete.

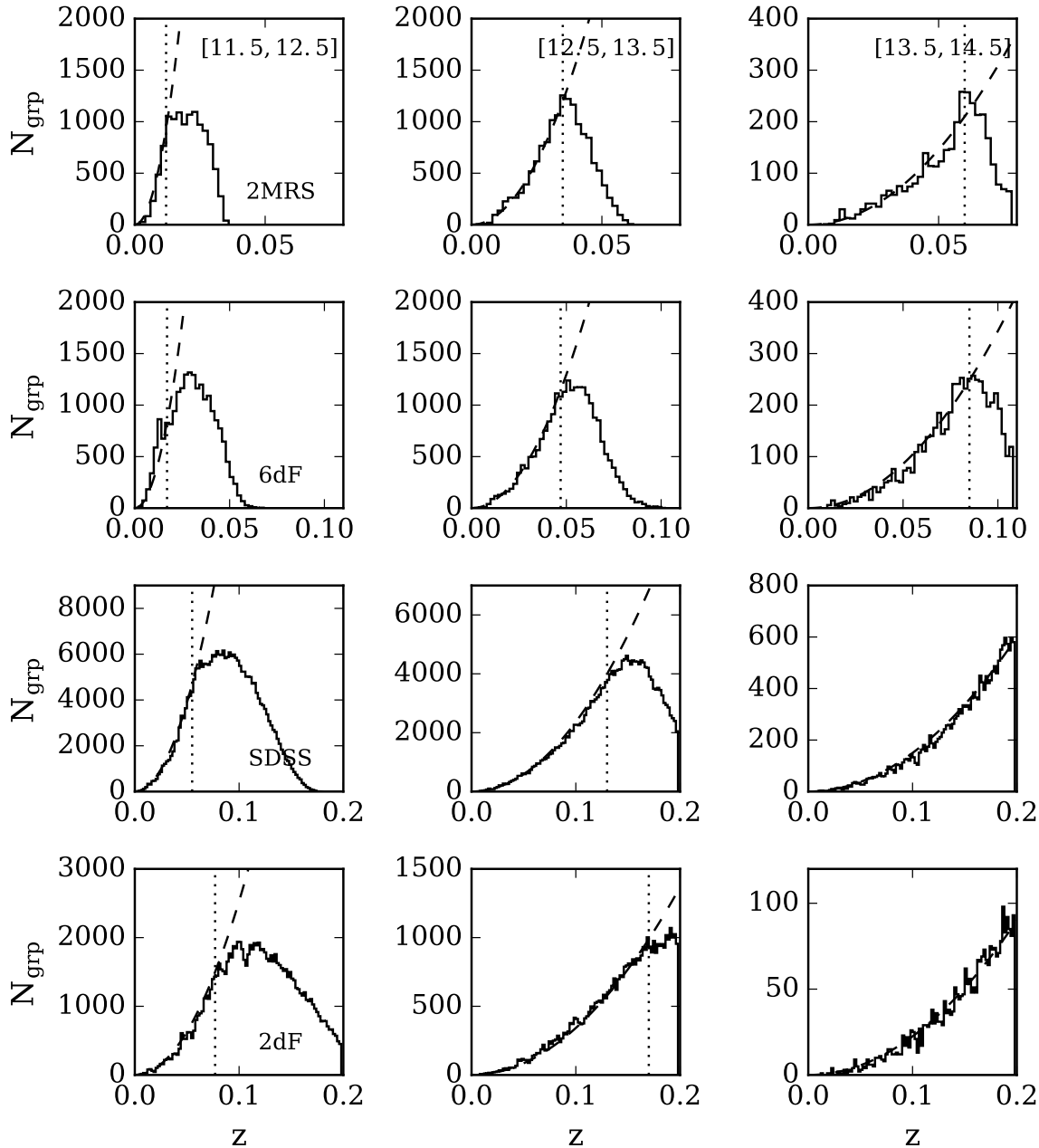


**Figure 7.** The number of halos as a function of redshift from the EAGLE simulation in several mass bins as indicated in the upper panels for each mock sample. The vertical dotted lines show the redshift limits to which the samples are complete for a given halo mass.

#### 4.4 Comparison with other group finders

As mentioned above, our group finder is built upon the group finders of Y05 and L16, but there are differences in details, especially in the halo mass proxies. Here we compare the performance of our group finder with respect to the earlier group finders by applying them to the same mock samples.

##### 4.4.1 Comparison with Yang et al.

In Yang et al. (2007) (Y07), the total group luminosity (group stellar mass) of member galaxies brighter than  $M_r =$

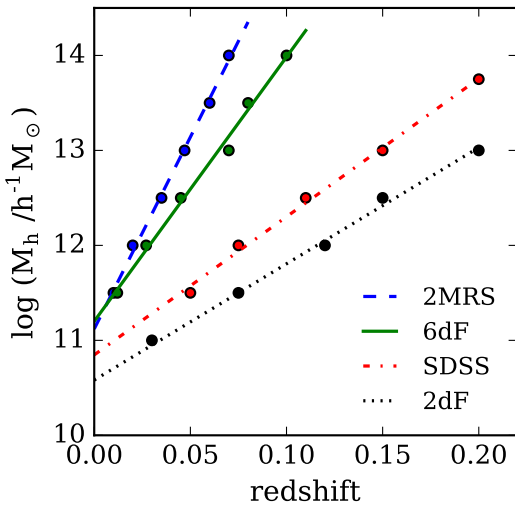
$-19.5 + 5 \log(h)$  in the  $r$ -band was used as the proxy of the halo mass. These group luminosity and stellar mass will be denoted as  $L_{19.5}$  and  $M_{*,19.5}$ , respectively. For galaxies at redshifts where the survey limit corresponds to an absolute magnitude brighter than the limit, Y07 used the observed luminosity function to account for the contribution to  $L_{19.5}$  from the missing galaxies due to the magnitude limit. However, as found in Y07, this correction introduces uncertainties in the group masses. This is not surprising given that most groups identified have only a few member galaxies even for the SDSS, and an extrapolation according to an average luminosity function is not expected to give an

**Table 3.** A summary of group catalogs constructed from the mock samples.<sup>a</sup>

Mock	Total groups	$N^b = 1$	$N = 2$	$N = 3$	$N \geq 4$
2MRS	30,124 (29,462)	25,160 (24,305)	3,128 (3,310)	881 (845)	955 (1002)
6dFGS	49,796 (48,496)	41,623 (39,938)	5,119 (5,427)	1,505 (1,477)	1,549 (1,654)
SDSS	473,303 (454,474)	397,300 (377,280)	49,166 (51,832)	13,937 (14,587)	14,846 (15,847)
2dFGRS	163,413 (156,825)	134,996 (126,670)	17,960 (18,548)	5,108 (5,740)	5,349 (5,867)

**Notes.**

- a. The numbers in parentheses are from the simulation.  
b. The number of member galaxies in a group.

**Figure 8.** Halo mass that is complete as a function of redshift for the mock samples of the simulation (circles), and linear fits to it (lines). We use the linear relation for abundance matching to assign halo masses to the mock groups.

accurate estimate of  $L_{19.5}$  ( $M_{*,19.5}$ ) for individual groups. Y07 found that the uncertainty introduced by this is larger than that introduced by the group finder itself, and is comparable to the intrinsic scatter in the true halo mass at a given  $L_{19.5}$  (or  $M_{*,19.5}$ ). As a more demanding test of our group finder against that of Y07, we restrict the mock sample to  $z \lesssim 0.09$ , the redshift limit to which the selection is complete to  $M_r = -19.5 + 5 \log(h)$  so that no extrapolation is needed in the group mass proxy used in Y07. The mock sample here is that constructed for the SDSS from the EAGLE simulation, as described in §2.5.

Figure 13 shows the group masses obtained from our group finder and the Y07 group finder with respect to the true halo masses of the simulation. When applying the Y07 group finder, the ranking of groups in  $M_{*,19.5}$  is used to assign group masses, while our group finder uses the halo mass proxy (stellar mass based) as described in §3.2. As one can see, our group finder matches the true halo masses with an accuracy slightly higher than that of Y07, with scatter typically of 0.15 – 0.2 dex. This indicates that Proxy-M and the GAP correction work as well as using  $M_{*,19.5}$  to assign halo masses to groups. However, had we included groups at  $z > 0.09$ , where extrapolation is needed in Y07’s group mass

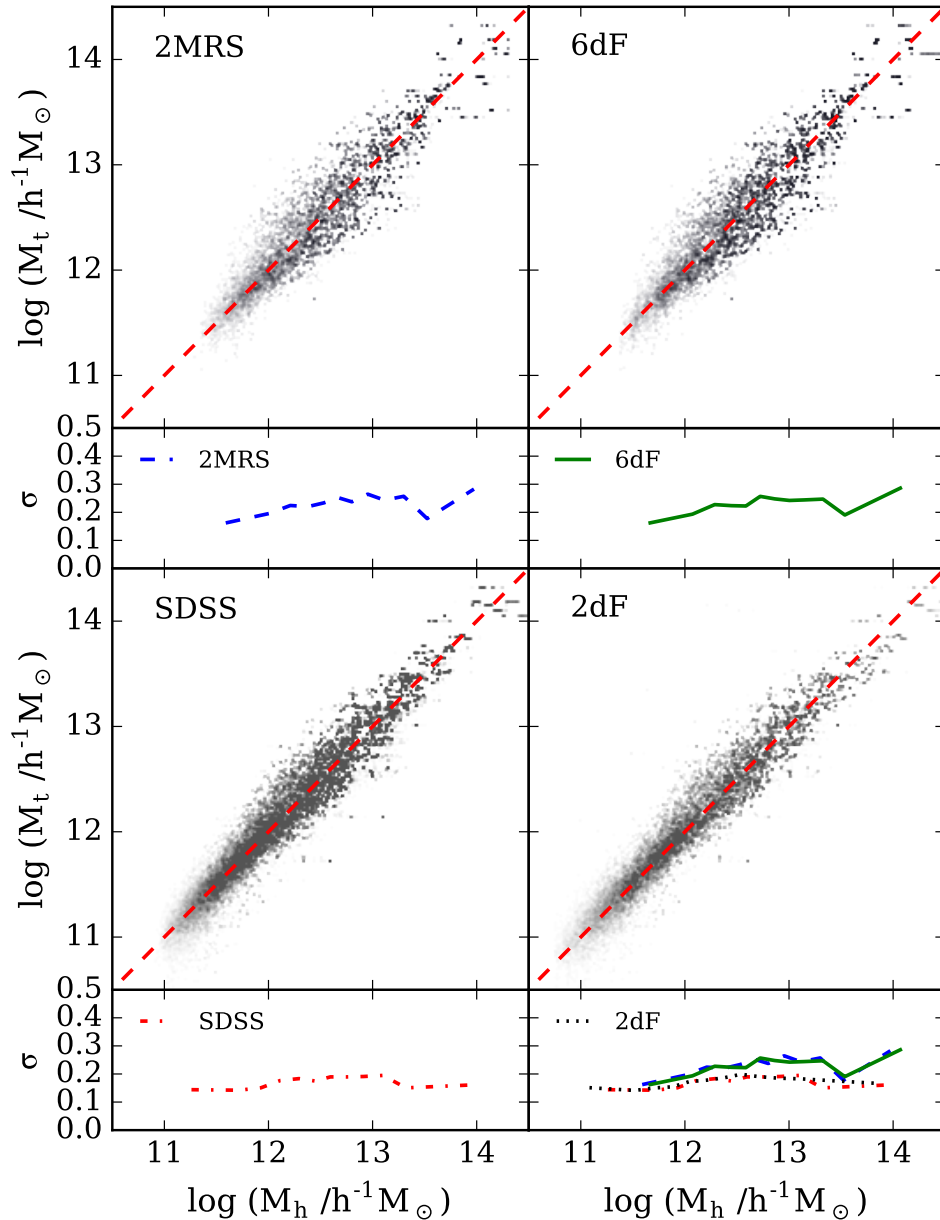
proxy, the scatter given by Y07 would become 0.25 – 0.3 dex while that given by our group finder remains at the level of 0.2 dex. In addition, our group finder performs equally well even for halos with masses as low as  $10^{11} h^{-1} M_\odot$ , about an order of magnitude lower than that reached by Y07. Many of these low mass halos contain only galaxies with  $M_r$  fainter than  $-19.5 + 5 \log h$ , which are not assigned halo masses in the original Y07 method. However, while the group finder of Y07 itself does not include these low-mass groups in the SDSS group catalog, halo mass assignment can be extended to lower masses by using a relation between halo mass and central galaxy, as given in, e.g., Yang et al. (2012). The number of groups identified by our group finder and the Y07 group finder are 180,835 and 184,833, of which 35,376 and 32,343 have more than one member, respectively. These are very close to the true number of halos of 177,013, of which 35,439 have more than one member.

Figure 14 shows the comparison of the two group finders in group completeness, contamination, and purity. For both of the group finders, the completeness decreases and the contamination increases with increasing halo masses, as we have seen in §4.3. The two group finders perform almost equally well in membership assignments.

#### 4.4.2 Comparison with Lu et al.

L16 developed and calibrated their group finder with their 2MRS mock samples constructed from an empirical conditional luminosity function model (see L16 for details). Here we apply our group finder and that of L16 to our own 2MRS mock sample, and make comparisons in their performances. For both of the group finders, we adopt the functional forms given by equation (9) and equation (10), and the corresponding best parameters for the GAP correction for groups of more than one member. Otherwise we follow the methodology of L16 as closely as possible to reproduce their group finder. The major difference between the two group finders is in the prescription for isolated galaxies. While our group finder uses Proxy-L to assign halo masses, we follow the prescription of L16 for their group finder. There are a total of 29,464 true halos, of which 5,158 have more than one member, and the number of groups identified by our group finder (by L16) are 30,118 (29,968), of which 4,980 (4,522) have more than one member. Furthermore, our group finder identifies 879 groups with three members and 364 with four members. The corresponding numbers by L16 are 888 and 362.

The group masses obtained by the two group finders are



**Figure 9.** Comparison between true halo mass (vertical axis) and group mass identified by our group finder (horizontal axis) using luminosity as the proxy of halo mass for the mock samples of 2MRS, 6dFGS, SDSS, and 2dFGRS constructed from the EAGLE simulation (see text for the sample selections). The small rectangular panels plot the scatter of true halo mass at given group mass.

compared to the true halo masses in Figure 15. One can see that our group finder reduces the overall scatter by  $\sim 0.1$  dex relative to that given by L16. As the two group finders work in a similar way for groups of more than one member, the improvement in our group finder is mainly due to a better mass proxy for groups containing only one member. Note also that the mass proxy used by L16 is calibrated with a mock catalog constructed from the observed conditional luminosity functions in the  $r$  band and scaled to the  $K$  band using abundance matching, while our mass proxies are calibrated with the EAGLE simulation. Part of the difference may also be due to the different calibrations. The scatter

we obtain here for the L16 group finder is very similar to that obtained in the original L16 paper from a completely different mock sample, suggesting that the test results are not particularly sensitive to the mock samples adopted for the test. This is also demonstrated in Appendix A, where it is shown that our group finder performs equally well for an independent mock sample constructed from an empirical model of galaxy formation.

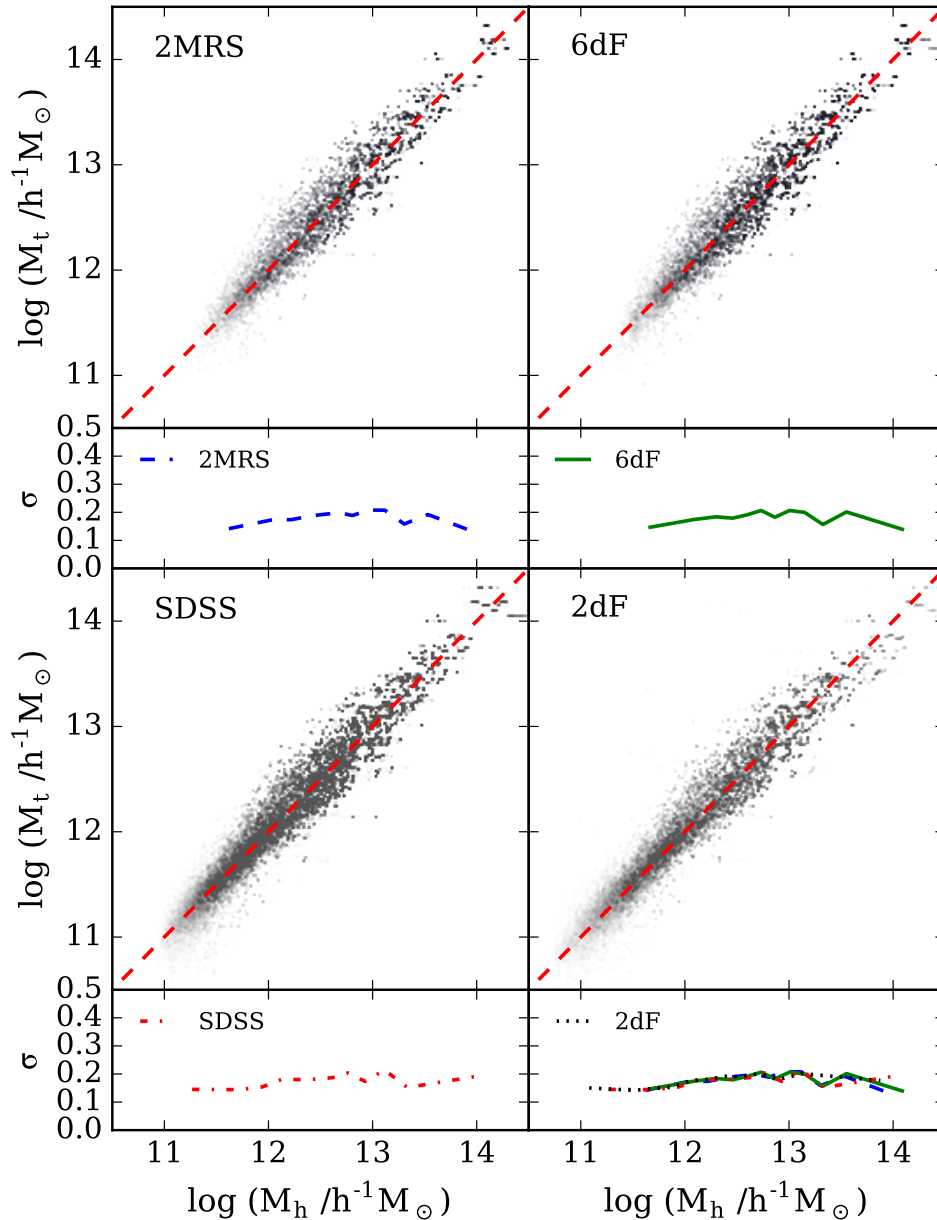


**Figure 10.** Same comparison as Figure 9 but using stellar mass as the proxy of halo mass.

## 5 THE GROUP CATALOGS

In this section, we present the group catalogs we construct by applying the group finder, as described in §3, to the observational samples described in §2. As mentioned earlier, we provide four catalogs for each observation sample:

- (i) a catalog constructed with galaxies that have spectroscopic redshifts, using Proxy-L to estimate halo masses;
- (ii) a catalog constructed with galaxies that have spectroscopic redshifts, using Proxy-M to estimate halo masses;
- (iii) a catalog constructed with all galaxies, using Proxy-L to estimate halo masses;
- (iv) and a catalog constructed with all galaxies, using Proxy-M to estimate halo masses.

For convenience we will use the name of the galaxy sample together with the halo mass proxy adopted to refer to a group catalog. For example, the catalogs constructed from the SDSS survey are referred to as SDSS(L), SDSS(M), SDSS+(L), and SDSS+(M), respectively. For brevity, the following presentations are mainly based on catalogs (i) and (ii), unless stated otherwise.

### 5.1 The catalogs and their basic properties

For SDSS and 2dFGRS, Proxy-L uses the  $r$ - and  $R$ -band luminosities, respectively, and Proxy-M uses the stellar masses of galaxies as described in §2.3 and §2.4. For 2MRS and 6dFGRS, Proxy-L is based on the  $K_s$ -band luminosities



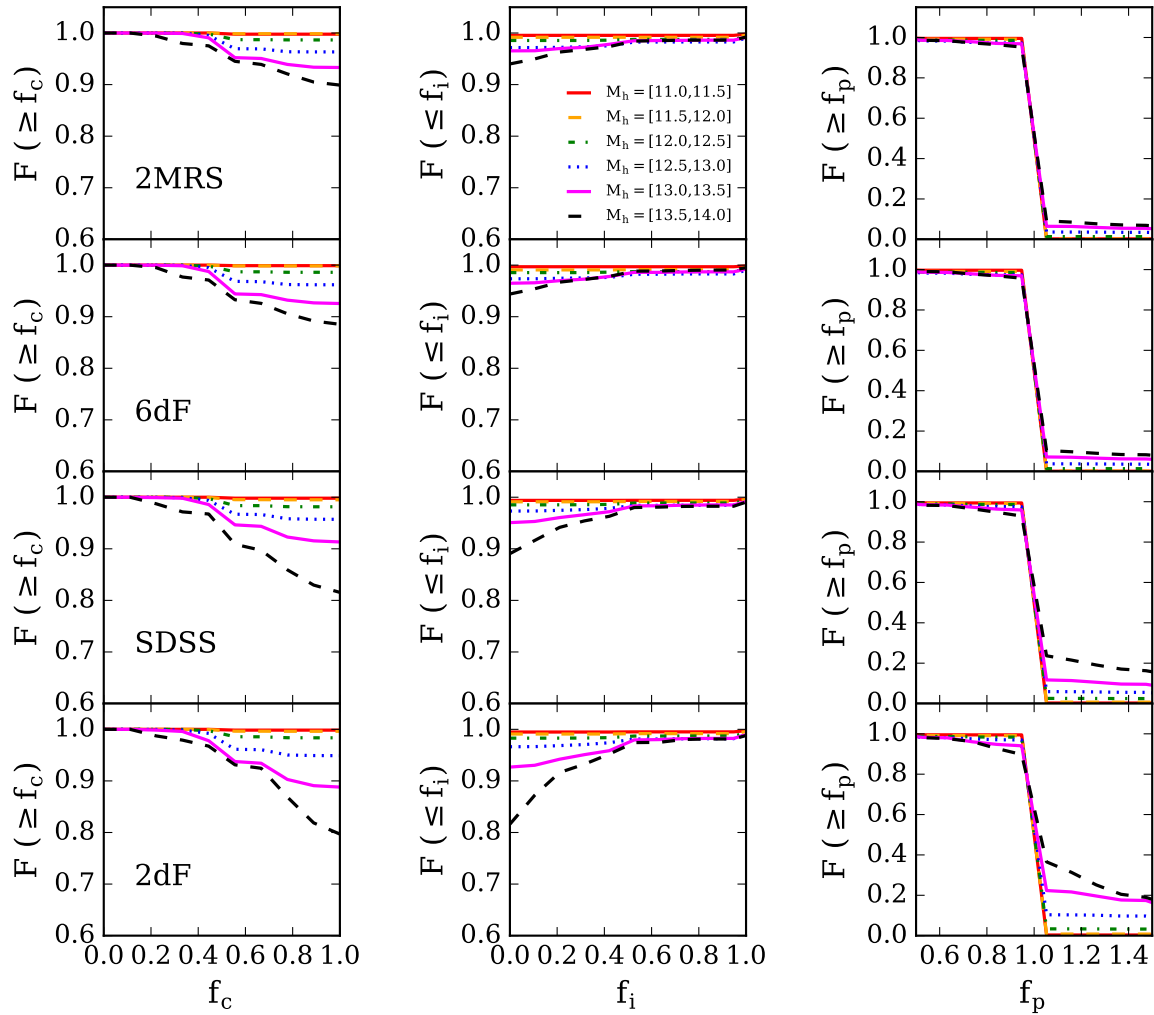


**Figure 11.** Membership assignments by the group finder applied to the mock samples, in terms of the completeness (left), contamination (middle), and purity (right). The vertical axis plots the cumulative fraction of the groups identified via the group finder, and the different lines are for halos of different masses as indicated.

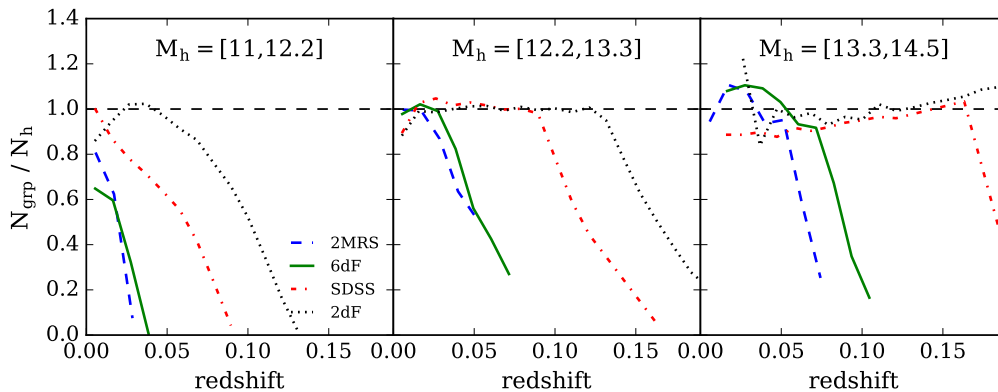


**Figure 12.** Global completeness, defined as the number of groups identified relative to the number of true halos, for the mock samples as a function of redshift for halos of different masses as indicated.

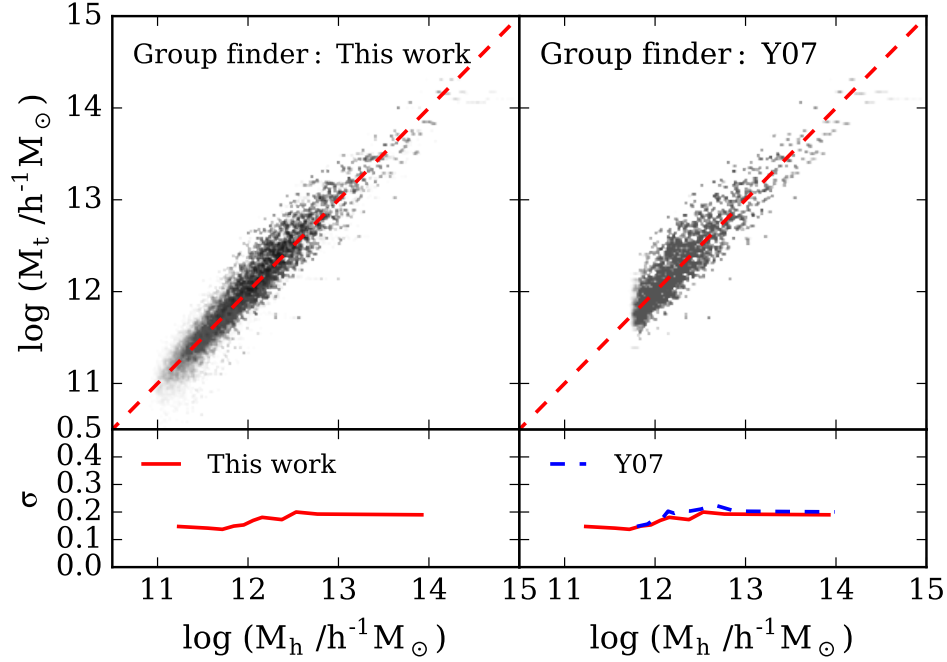


**Figure 13.** Comparison between the true halo mass of the EAGLE simulation and the group mass identified by our group finder (left) and by the group finder of Yang et al. (2007) (Y07; right) for the SDSS mock samples restricted to  $z \leq 0.09$ . The lower panels plot the scatter of the true halo masses at a given group mass.

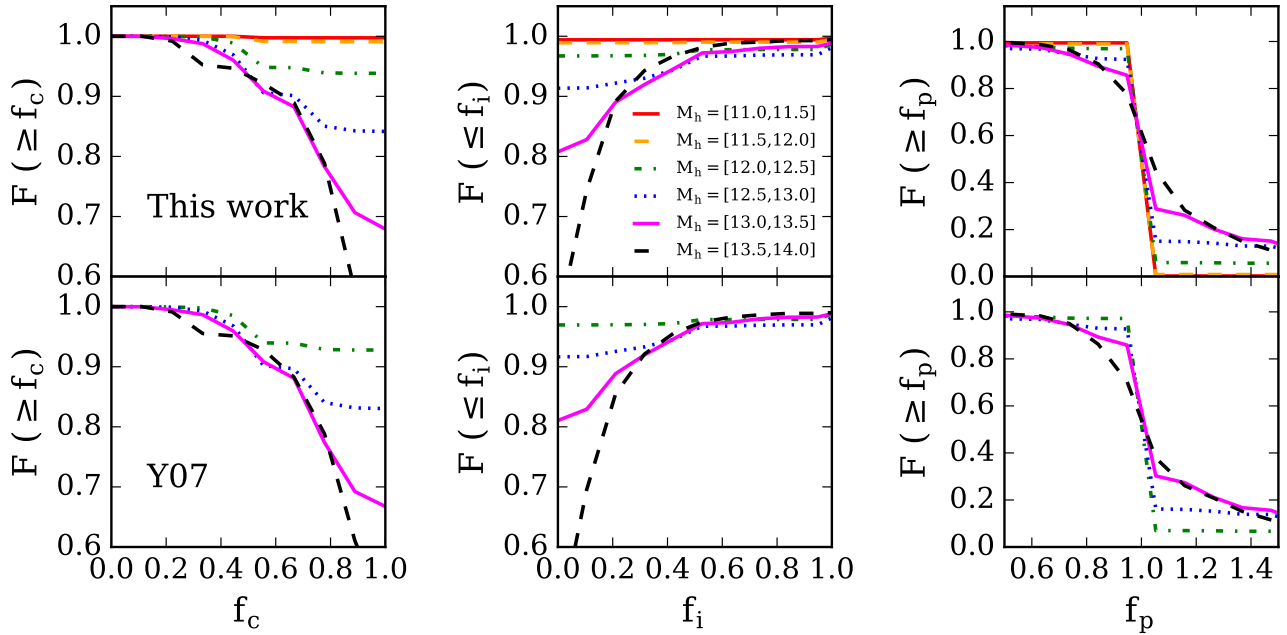


**Figure 14.** Comparison of membership assignment in terms of the completeness (left), contamination (middle), and purity (right) between our group finder (upper) and the group finder of Yang et al. (2007) (Y07; lower) for the same mock samples as Figure 13. The vertical axis plot the cumulative fraction of the groups, and the different lines are for haloes of different masses as indicated.

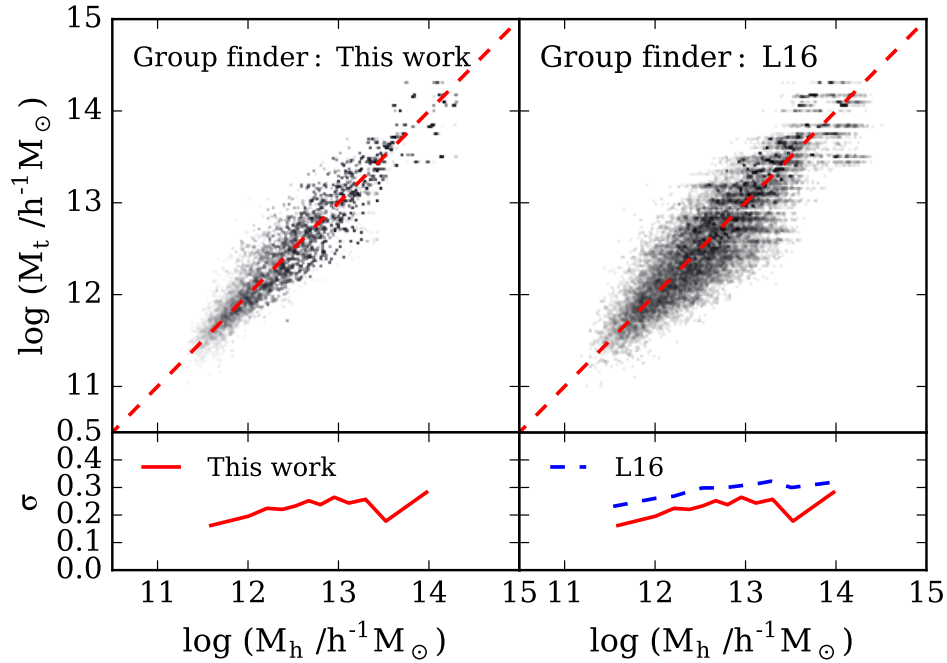


**Figure 15.** Comparison between the true halo mass of the EAGLE simulation and the group mass identified by our group finder (left) and by the group finder of Lu et al. (2016) (L16; right) for the 2MRS mock samples. The lower panels plot the scatter of the true halo masses at a given group mass.

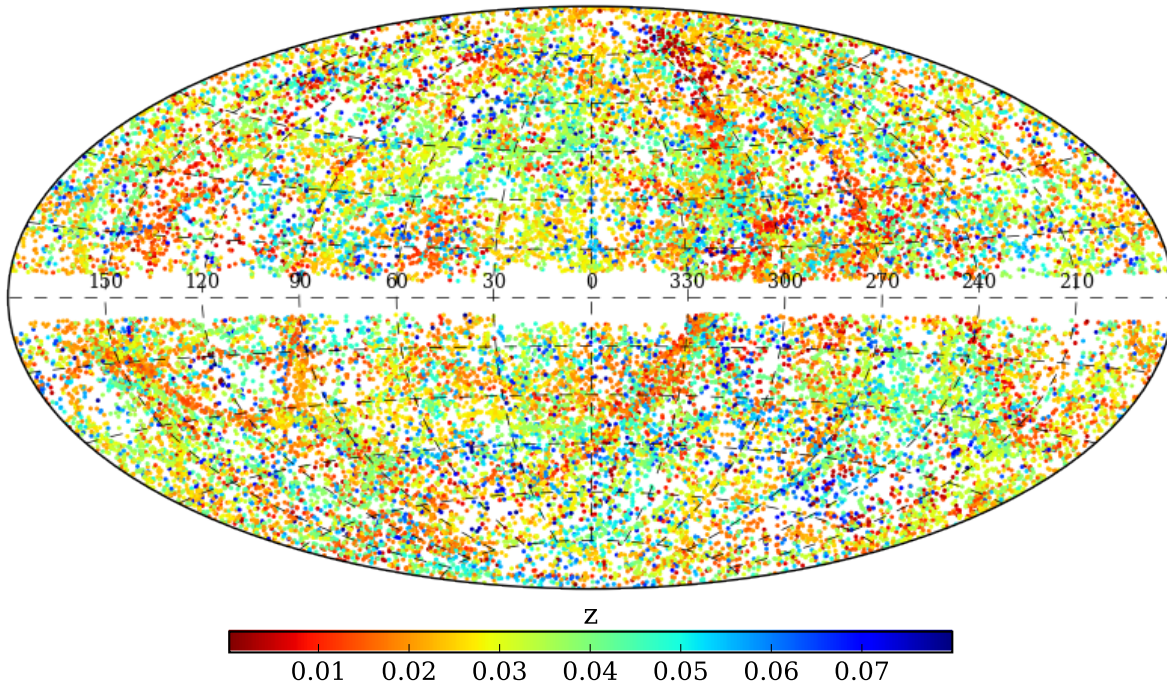


**Figure 16.** The group distributions in Galactic coordinates (Aitoff projection) of the 2MRS group catalog.

of galaxies. The Proxy-M for these two samples are based on the stellar masses obtained from the mean relation between the  $K_s$ -band luminosity and stellar mass from the EAGLE simulation. We use the same calibrations of the halo mass proxies as described in §3.2. Our tests show that it is not

necessary to re-calibrate the mass proxies for individual samples, as the outcomes with and without such a re-calibration converge in the end. This is expected, because our group finder uses the mass proxies only to rank group masses, and the halo masses are re-adjusted at the end of each iteration

**Table 4.** A summary of group catalogs.

Catalog	Total galaxies	Total groups <sup>a</sup>	Total groups with reliable mass	$N^b = 1$	$N \geq 2$	$M_h \geq 10^{14} M_\odot/h$	$M_h \geq 10^{13} M_\odot/h$
2MRS(L)	43,249	30,937	18,650	13,311	5,339	982	6,836
2MRS(M)	43,249	31,752	19,224	13,913	5,311	1,016	7,156
2MRS+(L)	44,310	31,804	18,731	13,275	5,456	984	6,877
2MRS+(M)	44,310	32,693	19,307	13,923	5,384	1,014	7,211
6dFGS(L)	62,987	46,676	17,907	11,126	6,781	1,004	6,919
6dFGS(M)	62,987	47,176	18,555	11,789	6,766	1,045	7,291
6dFGS+(L)	73,386	59,515	21,481	14,168	7,313	1,154	8,030
6dFGS+(M)	73,386	59,512	22,223	15,278	6,945	1,191	8,459
SDSS(L)	586,025	446,495	165,538	112,444	53,094	3,757	39,565
SDSS(M)	586,025	421,715	167,638	105,979	61,659	3,780	43,880
SDSS+(L)	600,458	453,927	164,694	107,066	57,528	3,712	39,464
SDSS+(M)	600,458	426,932	166,999	101,518	65,481	3,760	43,649
2dFGRS(L)	180,967	144,965	77,423	62,101	15,322	606	8,526
2dFGRS(M)	180,967	145,756	77,365	61,309	16,056	632	9,116
2dFGRS+(L)	189,101	147,757	77,861	59,606	18,255	634	8,553
2dFGRS+(M)	189,101	148,290	77,757	58,909	18,848	638	9,099

**Notes.**

<sup>a</sup> This includes groups without reliable halo mass assigned because halo mass is not complete at given redshift.

<sup>b</sup> The number of member galaxies in a group. This excludes groups without reliable halo mass assignment.

using abundance matching. In the tables and figures shown in this section, we exclude groups that are not assigned halo masses by abundance matching because of sample incompleteness at the given halo mass and redshift (see §4.2). In the catalogs, however, we include these groups (with a flag), and assign them masses according to the mean relation between the halo mass and the mass proxy obtained from the last iteration of the group finder.

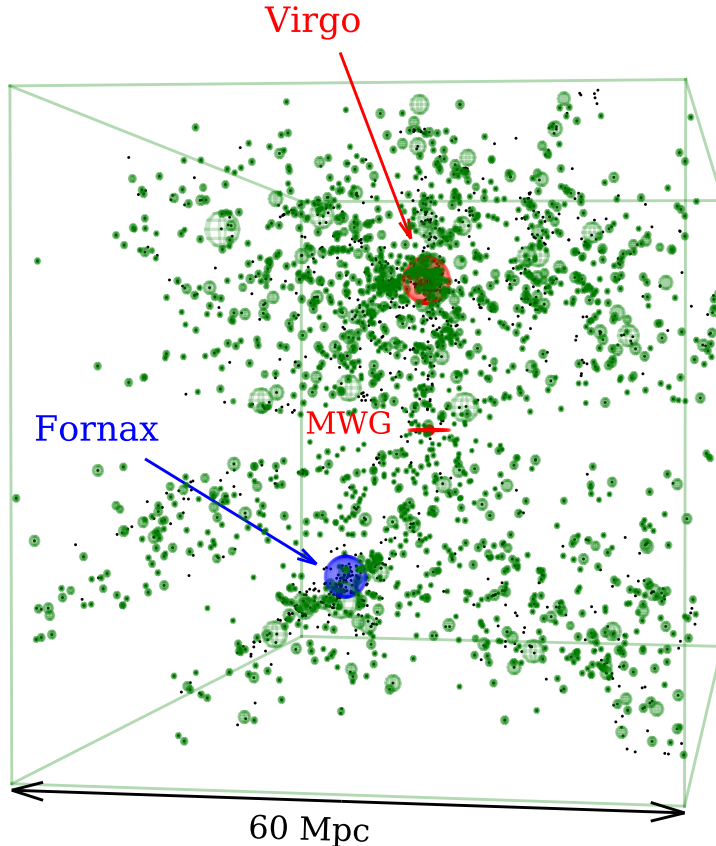
The distribution in the sky of the 2MRS groups selected by our group finder is shown in Figure 16, and Figure 17 shows the three dimensional distributions of galaxies and groups in the local Universe from the 2MRS catalogs. Also, the distributions of groups from different surveys in the same slices are compared in Figure 18.

Figure 19 compares the mass function of the halos from the group catalogs with the theoretical model of Sheth et al. (2001), which was used for abundance matching for the group finder. The good agreement between the observational data and the theoretical model is largely by design. However, the plots do show the halo-mass and redshift ranges covered by different samples, as well as the statistical uncertainties in the number densities of groups.

Table 4 lists the total number of groups, as well as the number of groups of given richness and halo masses selected from different samples. Figure 20 shows in more detail the distributions of groups with respect to richness (number of member galaxies), halo mass, and redshift. Note, again, that these distributions are obtained from groups for which halo

masses are complete at a given redshift, as shown in Figure 8. It is seen that the results from (L) and (M) catalogs are consistent with each other within the Poisson uncertainties. For comparison, we also show the results for the +(L) catalogs [the results for the +(M) catalogs are very similar] as the small dots. As one can see, results from the extended (+) catalogs are consistent with the non-extended catalogs, except for the 6dFGS which has the poorest completeness in spectroscopic redshifts. Also, some massive clusters in the catalogs have only one galaxy particularly for 2MRS and 6dFGS, because of their shallow depths that make satellites not observable.

Figure 21 compares halo masses (based on Proxy-M) for individual groups cross-identified between the group catalogs. While we do not present the comparison for the 2dFGRS because the number of such groups is small, we did check that the mean relation and scatter for the 2dFGRS are similar to those for the SDSS. We used the tolerances of angular separation less than  $10''$  and  $|\Delta z| \leq 10^{-3}$  for the cross-identifications. One can see that there is a very tight correlation in halo masses between the 2MRS and the 6dFGS group catalogs, while a larger dispersion of 0.2 – 0.3 dex is found between the 2MRS and SDSS, mainly because of the differences in the stellar mass estimates.



**Figure 17.** Three dimensional distribution of the 2MRS galaxies (black dots) and groups identified by the group finder (wire-framed green spheres with radii of  $r_{180}$ ) in the local Universe with the Milky Way at the center.

## 5.2 Comparison with other catalogs

Here we compare our catalogs with a number of other catalogs in the literature, including the 2MRS catalogs of L16 and Tully (2015) (T15), the SDSS catalog of Y07, and the 2dFGRS catalog of Y05.

### 5.2.1 Comparison of the 2MRS group catalog with L16

As mentioned earlier, L16 built a group catalog based on the same sample of the 2MRS galaxies as ours using a similar methodology. Figure 20 shows the comparison between the two catalogs in the number of groups as functions of richness, mass, and redshift, and it is clear that the two catalogs are in good agreements. We also checked the mass of individual haloes for groups that are cross-identified between the two catalogs, and found that our mass assignments are in general agreement with those of L16 with a typical dispersion of  $\sim 0.25$  dex between them.

As described earlier, our group finder is different from that of L16 in two ways. The first is that we re-calibrated the gap-based mass model of L16, so that the mass assigned to a group may be different from that of L16 even if it has the same membership of galaxies. Second, L16 used a ‘Gap limit’ prescription to assign masses for groups containing only one member (see §3.2.2), while our group finder does not. We believe that these are the sources of the dispersions and

discrepancies found in the comparison of halo mass between the two catalogs.

### 5.2.2 Comparison of the 2MRS group catalog with T15

Tully (2015) (T15) constructed a 2MRS group catalog using an empirical relation between halo mass (and the corresponding size and velocity dispersion) and a characteristic group luminosity to assign galaxies into groups. Figure 20 shows the comparison of our catalog with theirs in the number of groups as functions of richness, mass, and redshift. As T15 stated that their group catalog is less reliable outside the recession velocity range between 3,000 and 10,000  $\text{km s}^{-1}$ , we make comparisons only for the groups within the velocity range. One can see that T15 contains more massive clusters than our catalogs, while the richness and redshift distributions are in better agreements. T15 compared the mass function of their groups with a theoretical halo mass function and found that, although the shape of their group mass function is similar to that of the theoretical function, the normalization is about a factor of 4.6 higher. As mentioned above, T15 used an empirical model for their group masses, which is different from the mass proxies used in our group finder. Furthermore, their definition of halo masses is also different from ours. All these produce the differences seen between the two catalogs.

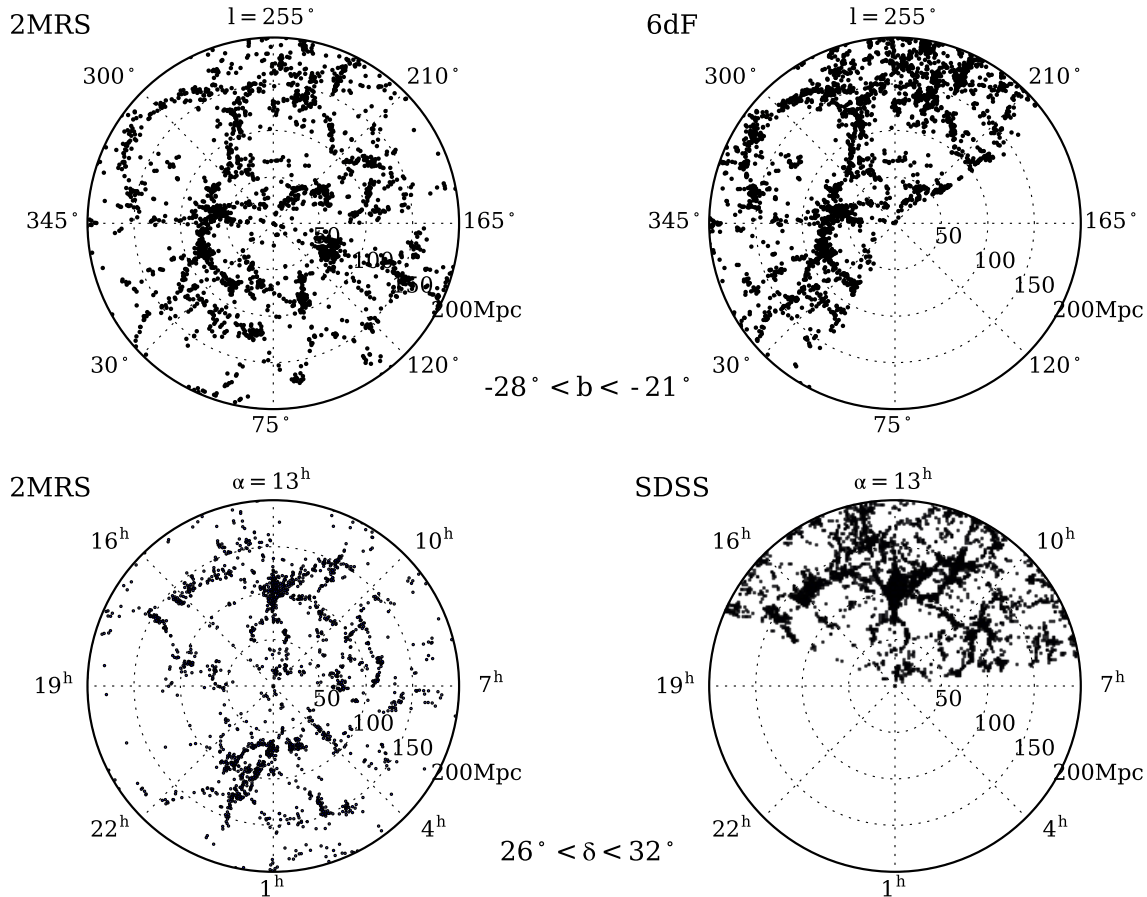


**Figure 18.** Comparison of the distribution of the groups constructed by the group finder in slices between different surveys. The upper and the lower panels show different slices as indicated.

### 5.2.3 Comparison of the SDSS group catalog with Yang et al.

Y07 built a group catalog of the SDSS DR7 galaxies. As we described earlier, their group finder is similar to ours in that it uses halo mass and velocity dispersion of groups identified to update galaxy memberships at each iteration until its iteration reaches convergence in the membership assignments. The main difference is that it uses a summed stellar mass (or luminosity) of member galaxies brighter than  $M_r = -19.5 + 5 \log h$  as a halo mass proxy. However, as the group catalogs are dominated by groups containing one galaxy (see Table 4), it results in no significant net difference except that our group catalog extends to lower mass. Figure 20 compares the SDSS group catalog of Y07 with that given by our group finder. The Y07 catalog contains smaller number of low-mass systems at relatively low redshifts, mainly because of the magnitude limit of  $M_r = -19.5 + 5 \log h$  adopted by Y07 in their halo mass proxy, which is brighter than the observational flux limit at  $z < \sim 0.09$ .

### 5.2.4 Comparison of the 2dFGRS group catalog with Yang et al.

Y05 also constructed a group catalog of the 2dFGRS galaxies. Again, their group finder is similar to ours but differs in that Y05 uses a summed stellar mass of member galaxies brighter than  $M_{b,J} = -18 + 5 \log h$  as a halo mass proxy instead of stellar mass (luminosity) of central galaxy and the  $n$ -th most massive (brightest) galaxy, which our group finder uses. The sample selection for the 2dFGRS is almost identical to our sample selection. Figure 20 shows comparisons between the two catalogs in the number of groups of given richness, mass, and redshift. The lower number of groups in Y05 in low-mass end and low-redshift is again because of the limit of  $M_{b,J} = -18 + 5 \log h$  used by Y07 for the halo mass proxy, which is brighter than the flux limit in the observation at  $z < \sim 0.12$ . Otherwise, the agreement between the two catalogs is reasonably good.

## 5.3 Contents of the catalogs

The galaxy and group catalogs constructed are available at <http://gax.sjtu.edu.cn/data/Group.html>. The group catalogs list the properties of groups, while the galaxy samples present not only the properties of galaxies but also their

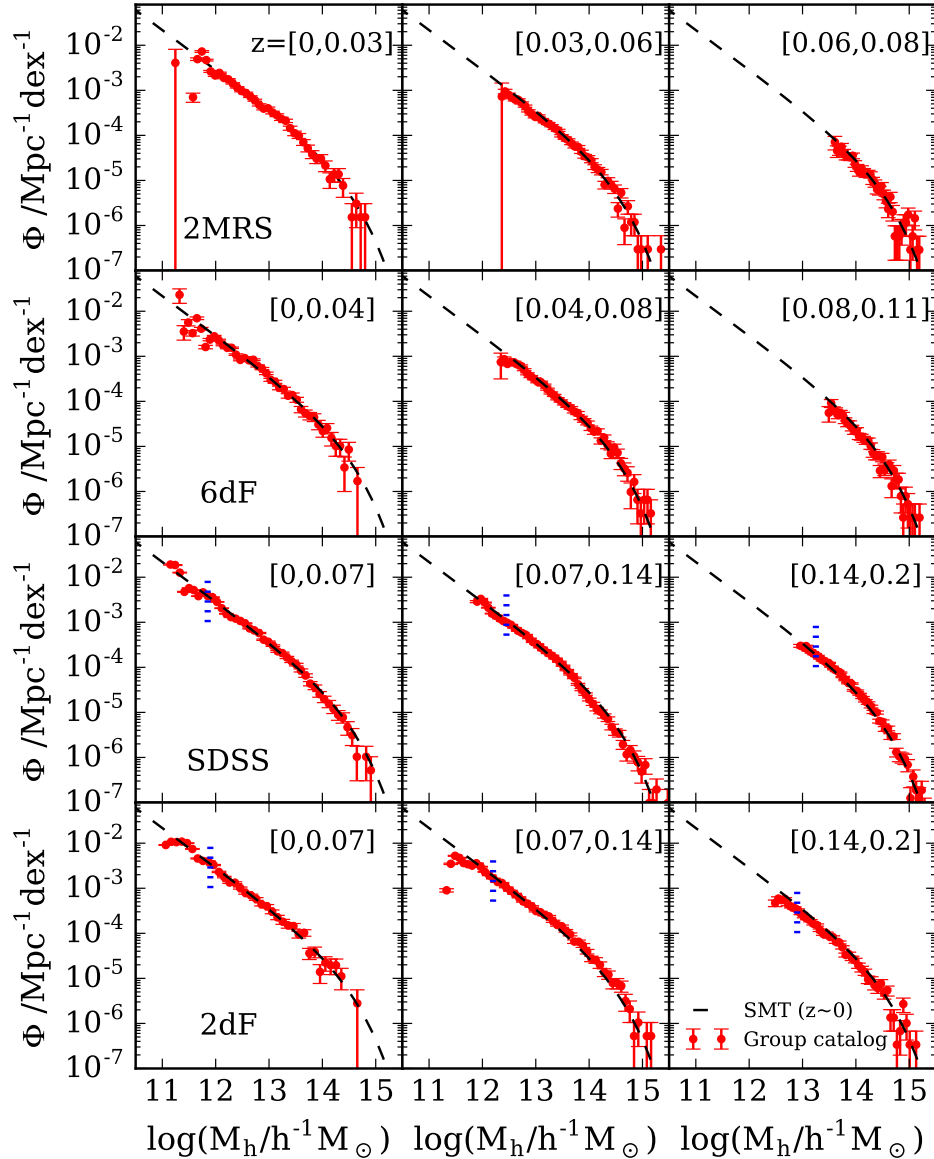


**Figure 19.** Halo mass functions of galaxy systems constructed based on the four surveys. The dashed lines are the theoretical mass function by Sheth et al. (2001), which we used for abundance matching for the group finder. The dotted short ticks in the lower two panels indicate the lower limits of the halo masses of the group catalogs by Yang et al. (2007) and Yang et al. (2005), respectively.

links to groups. Object indexes are also provided for galaxies so that one can identify them from the original galaxy catalogs. As mentioned above, there are four group catalogs for each galaxy sample, and so in total we provide 16 group catalogs, as summarized in Table 4. Tables 5 and 6 show the structures of the catalogs we provide, using the 2MRS as an example. In what follows we explain the different columns in more detail.

### 5.3.1 The group catalogs

The following items are provided for individual groups.

Column (1) group ID: an unique ID of a group within a given group catalog;

Column (2) cen ID: galaxy ID of the central galaxy of a group in the corresponding galaxy sample;

Column (3) ra (in degrees): right ascension (J2000) of the luminosity-weighted (for catalogs using Proxy-L) or mass-weighted (for catalogs using Proxy-M) group center;

Column (4) dec (in degrees): declination (J2000) of the group center;

Column (5)  $z$ : redshift of group center in the CMB rest-frame;

Column (6)  $\log(M_h/h^{-1}M_\odot)$ : 10-based logarithm of the halo mass of a group in units of  $h^{-1}M_\odot$ ;

Column (7)  $N_{\text{mem}}$ : number of member galaxies in a group;

Column (8)  $f_{\text{edge}}$ : the volume fraction that is not cut out

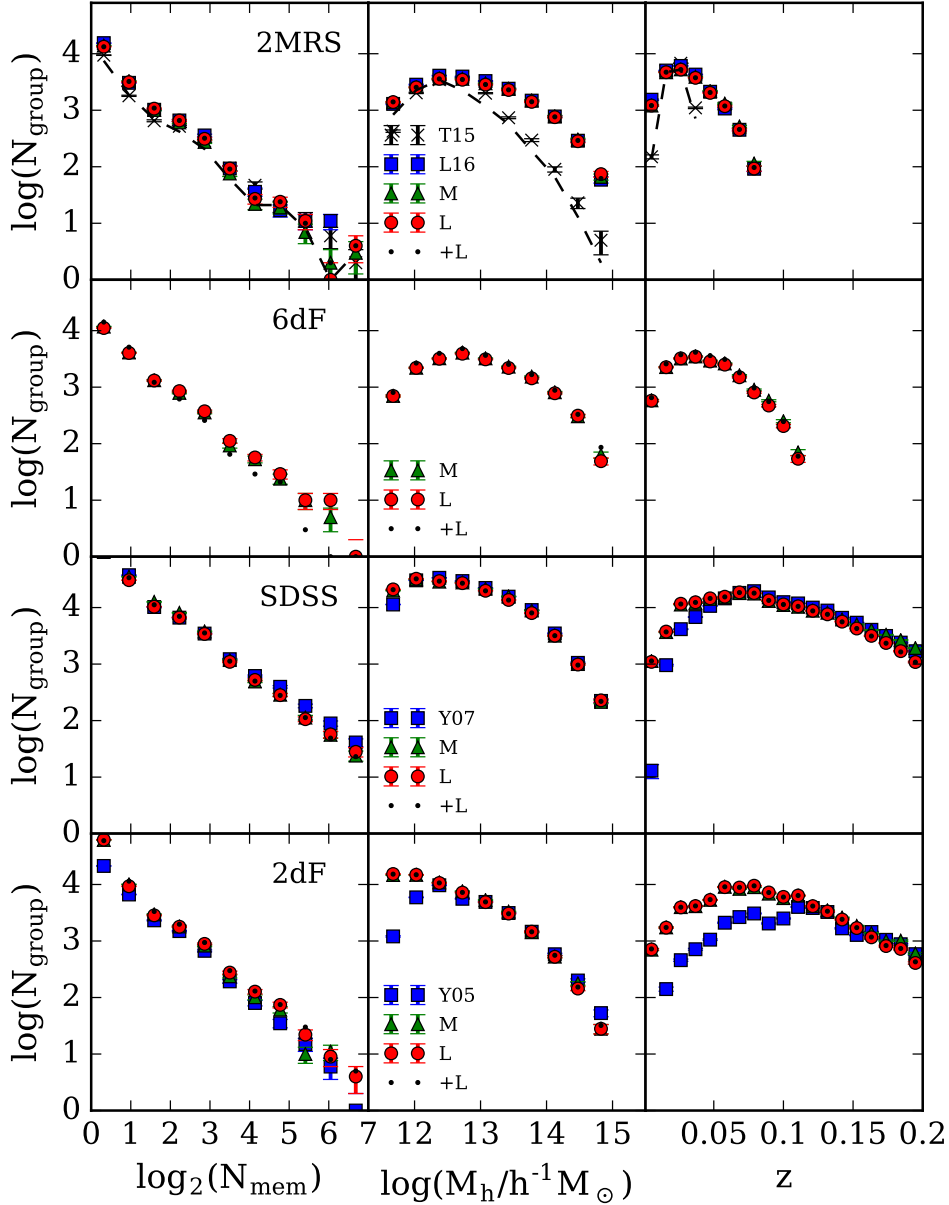


**Figure 20.** The number of groups as a function of the number of members, halo mass, and redshift for L (circle) and M (triangle) catalogs for each survey, compared with Tully (2015) (T15; cross) and Lu et al. (2016) (L16; square) for the 2MRS, with Yang et al. (2007) (Y07; square) for the SDSS, and with Yang et al. (2005) (Y05; square) for the 2dFGRS. The results from the +L catalogs (dots) are also shown for comparison. The T15 results (crosses) should be compared with the dashed lines, which are obtained by using only groups with recession velocities between 3,000 and 10,000 km s<sup>-1</sup>, within which the T15 sample is complete. The comparison is only made for groups that halo mass is complete at a given redshift. The error bars shown represent Poisson errors.

from the halo of a group (assumed to be spherical) by the survey boundary or mask;

Column (9) i-o: A flag that indicates whether a group is inside or outside the region of completeness for a given halo mass. For a group inside the completeness region (value = 1), mass is obtained directly from the abundance matching. For a group that is outside the completeness region (value = 0), mass is estimated using the re-

lation between the halo mass and its proxy from the last iteration of the group finder.

Column (10) known as: conventional name of a system, identified only for well-known massive clusters.

### 5.3.2 The galaxy catalogs

The following items are provided for individual galaxies.



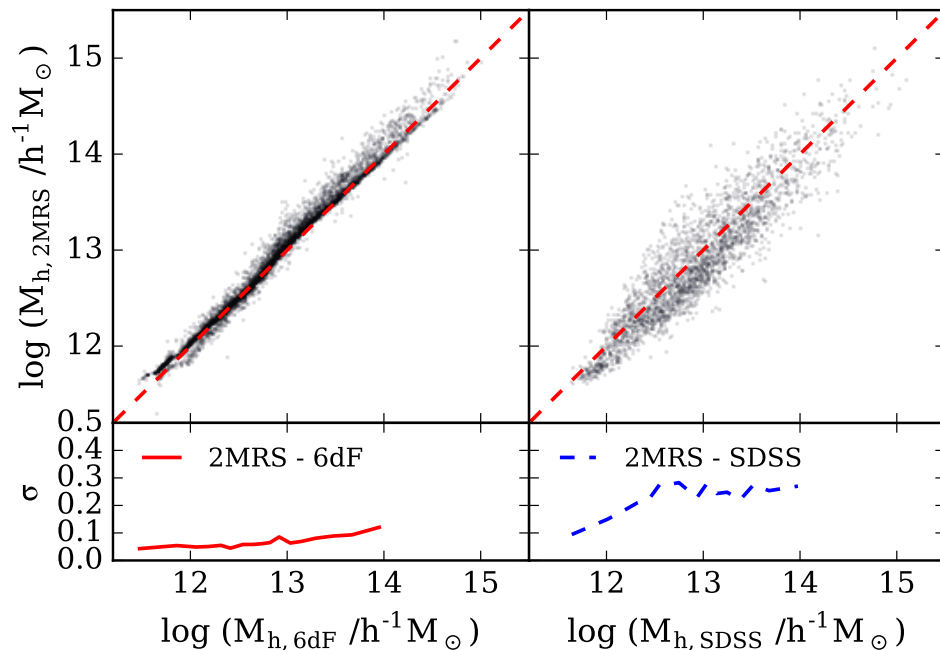


**Figure 21.** Comparison of halo masses (based on Proxy-M) for individual groups cross-identified between different group catalogs. We used the tolerances of  $\leq 10''$  and  $|\Delta z| \leq 10^{-3}$  for the cross-identification. The lower panels plot the scatter of the 2MRS halo masses at a given mass from the other catalogs.

**Table 5.** The 2MRS group catalog.<sup>a</sup>

(1)	(2)	(3)	(4)	(5)	(6)	(7)	(8)	(9)	(10)
group ID	cen ID	ra	dec	$z$	$\log(M_h/h^{-1}M_\odot)$	$N_{\text{mem}}$	$f_{\text{edge}}$	i-o	known as
		(deg)	(deg)						
1	15	187.74899	12.20402	0.00362	14.290	109	1.00	1	Virgo
2	486	243.52157	-60.79748	0.01663	14.366	106	1.00	1	Norma
3	530	49.47894	41.53527	0.01748	14.297	92	1.00	1	Perseus
4	672	194.81308	27.97206	0.02476	14.639	88	1.00	1	Coma
5	386	192.33072	-41.18290	0.01437	14.342	62	1.00	1	Centaurus
6	1094	258.01088	-23.30095	0.03030	14.758	52	1.00	1	Ophiuchus
7	18	53.13952	-35.56552	0.00492	14.097	48	1.00	1	Fornax
8	257	210.67554	-33.83448	0.01527	14.534	47	1.00	1	
9	608	17.31215	32.68145	0.01609	14.042	42	1.00	1	
10	432	207.35991	-30.43195	0.01628	14.220	41	1.00	1	

**Notes.**

a. The full catalog is available at <http://gax.sjtu.edu.cn/data/Group.html>.

**Table 6.** The 2MRS galaxy catalog.<sup>a</sup>

(1)	(2)	(3)	(4)	(5)	(6)	(7)	(8)	(9)	(10)	(11)	(12)	(13)	(14)
galaxy ID	survey ID	group ID	ra (deg)	dec (deg)	<i>l</i> (deg)	<i>b</i> (deg)	<i>z</i> <sub>CMB</sub>	<i>z</i> <sub>EDD</sub>	<i>z</i> <sub>comp</sub>	<i>z</i> <sub>src</sub>	dist <sub>NN</sub> (deg)	$\log(L/h^{-2}L_{\odot})$	$\log(M_{*}/h^{-2}M_{\odot})$
1	00424433 + 4116074	25128	10.68471	41.26875	121.1743	-21.57319	-0.00194	0.00018	1.0	0	0.0	10.644	10.286
2	00473313 - 2517196	1116	11.88806	-25.2888	97.36301	-87.96452	-0.00013	0.00086	1.0	0	0.0	10.771	10.432
3	09553318 + 6903549	345	148.88826	69.06526	142.0919	40.90022	0.00016	0.00085	1.0	0	0.0	10.749	10.406
4	13252775 - 4301073	299	201.36565	-43.01871	309.51639	19.41761	0.00267	0.00083	1.0	0	0.0	10.69	10.339
5	13052727 - 4928044	299	196.36366	-49.4679	305.27151	13.34017	0.00268	0.0	1.0	0	0.0	11.497	11.413
6	01335090 + 3039357	30717	23.4621	30.65994	133.61024	-31.33081	-0.00152	0.00021	1.0	0	0.0	9.439	9.201
7	09555243 + 6940469	345	148.96846	69.6797	141.40953	40.5671	0.00094	0.00082	1.0	0	0.0	10.394	10.02
8	03464851 + 6805459	29389	56.70214	68.09611	138.17259	10.57999	-0.0002	0.00053	1.0	0	0.0	10.12	9.754
9	13370091 - 2951567	5266	204.25383	-29.86576	314.58353	31.97269	0.00263	0.00115	1.0	0	0.0	10.691	10.34
10	12395949 - 1137230	12365	189.99789	-11.62307	298.46094	51.14923	0.00455	0.00228	1.0	0	0.0	11.146	10.906

**Notes.**

a. The full catalog is available at <http://gax.sjtu.edu.cn/data/Group.html>.

- Column (1) galaxy ID: unique ID of galaxies within each sample. This can be used to match galaxies across the galaxy and group catalogs;
- Column (2) survey ID: ID of galaxies from the original survey data release. This can be used to match galaxies across our catalogs and the original surveys;
- Column (3) group ID: ID of the group of which a galaxy is a member;
- Column (4) ra (in degrees): right ascension (J2000);
- Column (5) dec (in degrees): declination (J2000);
- Column (6)  $l$  (in degrees): Galactic longitude;
- Column (7)  $b$  (in degrees): Galactic latitude;
- Column (8)  $z_{\text{CMB}}$ : redshift in the CMB rest-frame. This is used for the group finder;
- Column (9)  $z_{\text{EDD}}$ : redshift for nearby galaxies based on the EDD distances. Otherwise equals to 0. This is only used for converting apparent magnitude to luminosity;
- Column (10)  $z_{\text{comp}}$ : redshift completeness along the direction on the sky where a galaxy lies;
- Column (11)  $z_{\text{src}}$ : a numerical value indicating the source of  $z_{\text{CMB}}$ . As the sources vary for different samples, please refer to the individual catalogs for more detailed descriptions;
- Column (12)  $\text{dist}_{\text{NN}}$ : angular separation to the nearest neighbor (deg) for galaxies that  $z_{\text{src}}$  is the nearest neighbor. Otherwise equals to 0.
- Column (13)  $\log(L/h^{-2}L_{\odot})$ : 10-based logarithm of the luminosity in units of  $h^{-2}L_{\odot}$ . Luminosities are in the  $K_s$ -band for 2MRS and 6dFGS, in the  $r$ -band for SDSS, and in the  $R$ -band for 2dFGRS.  $K$ - and evolutionary corrections to  $z = 0.1$  are made following [Lavaux & Hudson \(2011\)](#) (for 2MRS and 6dFGS) and [Poggianti \(1997\)](#) (for SDSS and 2dFGRS). All quantities are calculated with the assumption of the WMAP9 cosmology;
- Column (14)  $\log(M_*/h^{-2}M_{\odot})$ : 10-based logarithm of the stellar mass in units of  $h^{-2}M_{\odot}$ . Please refer to the relevant sections for how the stellar masses are estimated in different samples;
- Column (15) color: provided only for SDSS ( $g - r$ ) and 2dFGRS ( $b_J - R$ ).

## 6 SUMMARY

In this paper, we have constructed group catalogs from four large redshift surveys in the low- $z$  universe: the 2MRS, 6dFGS, SDSS, and 2dFGRS. The groups are identified with a halo-based group finder that is based on the group finders developed in Y05, Y07 and L16 but has improved halo mass assignments that can be applied uniformly to various observations. The group finder uses stellar mass or luminosity of central galaxies combined with the luminosity/stellar mass gap between the central galaxy and the  $n$ -th brightest/most massive satellite as halo mass proxies. It assigns galaxies into groups using halo properties, such as halo size and velocity dispersion, and iterates with updated halo properties until the membership converges. We use an abundance matching technique to assign final halo masses to individual groups se-

lected. For groups that are not assigned mass by abundance matching, due to the fact that they are outside the redshift limit within which groups of a given mass is complete, halo masses are assigned based on the mean relation between halo mass and its proxy obtained from the last iteration of the group finder.

We have used realistic mock galaxy samples constructed from a hydrodynamical simulation (EAGLE) to test the performance and to calibrate our group finder, and used another set of mock samples constructed from an empirical model of galaxy formation as an independent check. The tests showed that our group finder can find  $\sim 95\%$  of the ‘true’ member galaxies for about 95% (85%) of the groups for the 2MRS and 6dFGS samples (for the SDSS and 2dFGRS samples), with better membership assignment for lower mass halos. The tests on mock samples also showed that the halo masses of individual groups estimated by the group finder are consistent with the true halo masses, with scatter of  $\sim 0.2$  dex. The scatter in the estimated mass - true mass relation obtained here for the SDSS sample is similar to Y07, but it extends uniformly to halo masses that are about 0.7 dex lower.

We have constructed group catalogs by applying our group finder to the real redshift surveys of galaxies. From each survey, two samples of galaxies are constructed, one using only galaxies with spectroscopic redshifts, and the other using all galaxies, including the ones with redshifts estimated from nearest neighbors or from photometry (photometric redshifts). For each galaxy sample, two group catalogs are constructed, one using the luminosity-based halo mass proxy (Proxy-L) and the other using the stellar mass-based halo mass proxy (Proxy-M). Thus, we provide a total of 16 group catalogs, four different sets of catalogs for each of the four surveys. A summary of the all the group catalogs and how to use them are presented in §5. We have also described some of the basic properties of the group catalogs, such as the distributions in richness, redshift, and mass. Comparisons are made with other similar catalogs in the literature.

It should be noted that the group catalogs constructed are cosmology dependent, and we have adopted WMAP9 cosmology in the present paper. This dependence comes from both the properties of dark matter halos (halo size and velocity dispersion as functions of halo mass) adopted in grouping galaxies into common halos, and the halo mass function used in abundance matching. However, as demonstrated in Y07, the grouping of galaxies into groups is not sensitive to the cosmological model, unless the adopted model is very different from that favored by current observations. The cosmology dependence in the halo mass assignments is also not a significant problem, as it is straightforward to convert the masses to other cosmologies with abundance matching.

The data published in this paper are available at the website: <http://gax.sjtu.edu.cn/data/Group.html>.

## ACKNOWLEDGEMENTS

This work is supported by the 973 Program (No. 2015CB857002) and the national science foundation of China (grant Nos. 11233005, 11621303, 11522324, 11421303, 11503065). HJM acknowledges the support from NSF AST-1517528 and NSFC-11673015. SHL thanks his wife, Hyeji

Jung, who took care of their kids mostly alone during writing this paper. We thank Hong Guo for useful discussions regarding the fiber-collision galaxies as well as providing the catalog of the fiber-collision galaxies in the SDSS DR7 that have redshift measured in the later data release, Shiyin Shen for providing the newest LAMOST redshifts prior to their publication, the referee, Brent Tully, for comments that improved this paper, and the Virgo Consortium for making the EAGLE simulation data available. The EAGLE simulations were performed using the DiRAC-2 facility at Durham, managed by the ICC, and the PRACE facility Curie based in France at TGCC, CEA, Bruyères-le-Châtel. We also acknowledge the use of the data products from the 2MASS, which is a joint project of the University of Massachusetts and the Infrared Processing and Analysis Center/California Institute of Technology, funded by the National Aeronautics and Space Administration and the National Science Foundation. The Wide Field Astronomy Unit at the Institute for Astronomy, Edinburgh is acknowledged for archiving the 2MPZ catalog, which can be accessed at <http://surveys.roe.ac.uk/ssa/TWOMPZ>. Support for the development of the content for the EDD database is provided by the National Science Foundation under Grant No. AST09-08846. This publication also makes use of the data products from the 2M++ catalog, the Final Release of the 6dFGS (available at <http://www-wfau.roe.ac.uk/6dFGS/>), and the KIAS VAGC. We acknowledge the 2dFGRS team for the survey and for making their catalogs available, which was made possible through the dedicated efforts of the staff of the Anglo-Australian Observatory, both in creating the instrument and in supporting the survey observations. Funding for the Sloan Digital Sky Survey IV has been provided by the Alfred P. Sloan Foundation, the U.S. Department of Energy Office of Science, and the Participating Institutions. SDSS-IV acknowledges support and resources from the Center for High-Performance Computing at the University of Utah. The SDSS web site is [www.sdss.org](http://www.sdss.org). SDSS-IV is managed by the Astrophysical Research Consortium for the Participating Institutions of the SDSS Collaboration including the Brazilian Participation Group, the Carnegie Institution for Science, Carnegie Mellon University, the Chilean Participation Group, the French Participation Group, Harvard-Smithsonian Center for Astrophysics, Instituto de Astrofísica de Canarias, The Johns Hopkins University, Kavli Institute for the Physics and Mathematics of the Universe (IPMU) / University of Tokyo, Lawrence Berkeley National Laboratory, Leibniz Institut für Astrophysik Potsdam (AIP), Max-Planck-Institut für Astronomie (MPIA Heidelberg), Max-Planck-Institut für Astrophysik (MPA Garching), Max-Planck-Institut für Extraterrestrische Physik (MPE), National Astronomical Observatories of China, New Mexico State University, New York University, University of Notre Dame, Observatório Nacional / MCTI, The Ohio State University, Pennsylvania State University, Shanghai Astronomical Observatory, United Kingdom Participation Group, Universidad Nacional Autónoma de México, University of Arizona, University of Colorado Boulder, University of Oxford, University of Portsmouth, University of Utah, University of Virginia, University of Washington, University of Wisconsin, Vanderbilt University, and Yale University.

## REFERENCES

- Abell G. O., 1958, *ApJS*, 3, 211  
 Abell G. O., Corwin H. G. Jr., Olowin R. P., 1989, *ApJS*, 70, 1  
 Albareti F. D. et al., arXiv:1608.02013  
 Bell E. F., McIntosh D. H. Katz, N., Weinberg M. D., 2003, *ApJS*, 149, 289  
 Bennett C. L. et al., 2003, *ApJS*, 148, 1  
 Berlind A. A. et al., 2006, *ApJS*, 167, 1  
 Bilicki M., Jarrett T. H., Peacock J. A., Cluver M. E., Steward L., 2014, *ApJS*, 210, 9  
 Bruzual G., Charlot S., 2003, *MNRAS*, 344, 1000  
 Butcher H., Oemler A. Jr., 1978, *ApJ*, 226, 559  
 Butcher H., Oemler A. Jr., 1984, *ApJ*, 285, 426  
 Chabrier G., 2003, *PASP*, 115, 763  
 Choi Y.-Y., Han D.-H., Kim S. S., 2015, *JKAS*, 43, 191  
 Cohen M., Wheaton Wm. A., Megeath S. T., 2003, *AJ*, 126, 1090  
 Colless M. et al., 2001, *MNRAS*, 328, 1039  
 Crain R. A. et al., 2015, *MNRAS*, 450, 1937  
 Crook A. C. et al., 2007, *ApJ*, 655, 790  
 Dawson K. S. et al., 2013, *AJ*, 145, 10  
 Dressler A., 1980, *ApJ*, 236, 351  
 Duarte M., Mamon G. A., 2015, *MNRAS*, 453, 3848  
 Eke V. R. et al., 2004, *MNRAS*, 348, 866  
 Finkbeiner D. P. et al., 2016, *ApJ*, 822, 66  
 Goto T., 2005, *MNRAS*, 359, 1415  
 Guo H. et al., 2015, *MNRAS*, 453, 4368  
 Huchra J. P., Geller M. J., 1982, *ApJ*, 257, 423  
 Huchra J. P., Davis M., Latham D., Tonry J., 1983, *ApJS*, 52, 89  
 Huchra J. P. et al., 2012, *ApJS*, 199, 26  
 Jones D. H. et al., 2004, *MNRAS*, 355, 747  
 Jones D. H., Saunders W., Read M., Colless M., 2005, *PASA*, 22, 277  
 Jones D. H. et al., 2009, *MNRAS*, 399, 683  
 Lavaux G., Hudson M. J., 2011, *MNRAS*, 416, 2840  
 Lu Z., Mo H. J., Lu Y., Katz N., Weinberg M. D., van den Bosch F. C., Yang X., 2014, *MNRAS*, 439, 1294  
 Lu Z., Mo H. J., Lu Y., Katz N., Weinberg M. D., van den Bosch F. C., Yang X., 2015, *MNRAS*, 450, 1604  
 Lu Y., Yang X., Shi F., Mo H. J., Tweed D., Wang H., Zhang Y., Li S., Lim S. H., 2016, *ApJ*, 832, 39  
 Luo A.-L. et al., 2015, *RAA*, 15, 1095  
 McAlpine S. et al., 2016, *Astronomy and Computing*, 15, 72  
 McIntosh D. H., Bell E. F., Weinberg M. D., Katz N., 2006, *MNRAS*, 373, 1321  
 Mo H. J., White S. D. M., 1996, *MNRAS*, 282, 347  
 Mo H. J., van den Bosch F. C., White S. D. M., 2010, *Galaxy Formation and Evolution*. Cambridge University Press, New York, NY  
 Planck Collaboration et al., 2014, *A&A*, 571  
 Poggianti B. M., 1997, *A&AS*, 122, 399  
 Postman M., Geller M. J., 1984, *ApJ*, 281, 95  
 Schaye J. et al., 2015, *MNRAS* 446, 521  
 Schlegel D. J., Finkbeiner D. P., Davis, M., 1998, *ApJ*, 500, 525  
 Shen S.-Y. et al., 2016, *RAA*, 16, 43  
 Sheth R. K., Mo H. J., Tormen, G., 2001, *MNRAS*, 323, 1  
 Skrutskie M. F. et al., 2006, *AJ*, 131, 1163  
 Tully R. B., Rizzi L., Shaya E. J., Courtois H. M., Makarov

- D. I., Jacobs B. A., 2009, *AJ*, 138, 323
- Tully R. B., 2015, *AJ*, 149, 171
- Wang H., Mo H. J., Jing Y. P., Guo, Y., van den Bosch F. C., Yang X., 2009, *MNRAS*, 394, 398
- Wang H., Mo H. J., Yang X., van den Bosch F. C., 2013, *ApJ*, 772, 63
- Wang H., Mo H. J., Yang X., Jing Y. P., Lin W. P., 2014, *ApJ*, 794, 94
- Wang H. et al., 2016, *ApJ*, 831, 164
- Weinmann S. M., van den Bosch F. C., Yang X., Mo H. J., 2006, *MNRAS*, 366, 2
- Yang X., Mo H. J., van den Bosch F. C., Jing Y. P., 2005, *MNRAS*, 356, 1293
- Yang X., Mo H. J., van den Bosch F. C., Pasquali A., Li C., Barden M., 2007, *ApJ*, 671, 153
- Yang X., Mo H. J., van den Bosch F. C., Zhang Y., Han J., 2012, *ApJ*, 752, 41
- Zhao D. H., Jing Y. P., Mo H. J., Börner G., 2009, *ApJ*, 707, 354
- Zwicky F., Herzog E., Wild P., Karpowicz M., Kowal C. T., 1961-1968, *Catalogue of Galaxies and Clusters of Galaxies* (Pasadena: California Institute of Technology)

## A TESTING THE GROUP FINDER WITH MOCK SAMPLES CONSTRUCTED USING AN EMPIRICAL MODEL

To further check the consistency of our group finder, which is calibrated with galaxies in the EAGLE simulation, we have applied it to another set of mock samples constructed using the empirical model of galaxy formation described in [Lu et al. \(2015\)](#), which is based on [Lu et al. \(2014\)](#). The tests we have made are the same as those with the EAGLE mock samples presented in §4, using exactly the same methods described in §3. To do this, we first applied the empirical model to the merger trees extracted from the EAGLE to assign stellar masses to galaxies. As an example, [Figure A1](#) compares the true halo masses from the EAGLE simulation with the final group masses obtained by applying our group finder to the mock samples thus constructed. The scatter in the halo mass comparison is around 0.2 dex, very similar to what was found in [Figure 10](#) except for the very massive end which shows slightly larger scatter. This demonstrates that the performance of our group finder is not sensitive to the details of how galaxies form in dark matter halos, as represented by the differences between the EAGLE and the empirical model of [Lu et al. \(2015\)](#).

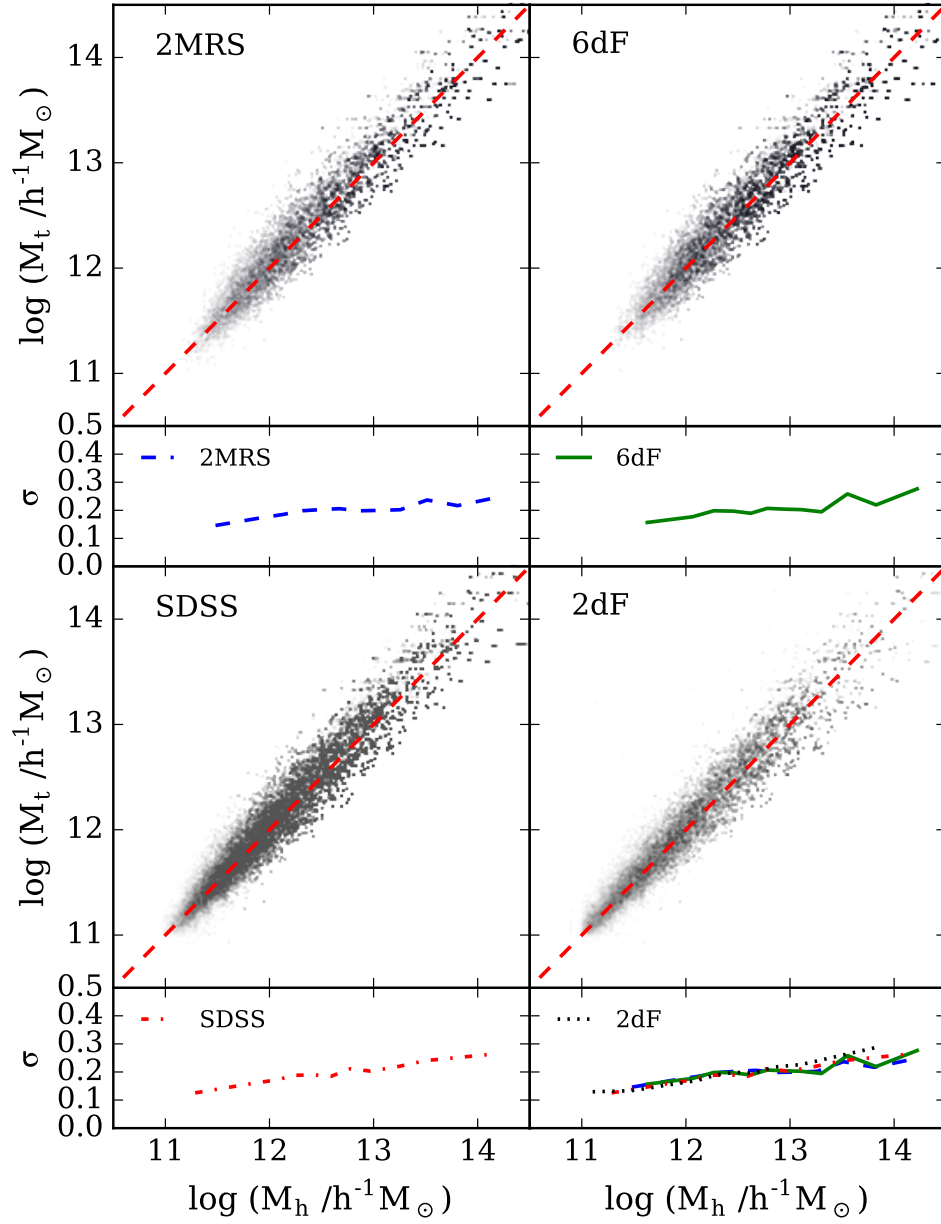


**Figure A1.** Comparison between the true halo mass (vertical axis) and the group mass identified by our group finder (horizontal axis) using stellar mass as the proxy of halo mass for the mock samples of 2MRS, 6dFGS, SDSS, and 2dFGRS. Here mock samples are constructed by applying the empirical model of [Lu et al. \(2015\)](#) to the halo merger trees extracted from the EAGLE simulation. The small rectangular panels plot the scatter of the true halo masses at given group mass.